A Critical Review on Condensation Heat Transfer in Microchannels and Minichannels

M. M. Awad[1]
Faculty of Engineering,
Mechanical Power Engineering Department,
Mansoura University,
Mansoura 35516, Egypt
e-mail: m_m_awad@mans.edu.eg

A. S. Dalkiliç
Heat and Thermodynamics Division,
Department of Mechanical Engineering,
Yildiz Technical University (YTU),
Yildiz, Besiktas,
Istanbul 34349, Turkey
e-mail: dalkilic@yildiz.edu.tr

S. Wongwises
Fluid Mechanics,
Thermal Engineering and Multiphase Flow
Research Laboratory (FUTURE),
Department of Mechanical Engineering,
King Mongkut's University of Technology
Thonburi (KMUTT), Bangmod,
Bangkok 10140, Thailand
e-mail: somchai.won@kmutt.ac.th

Condensation in microchannels and minichannels is widely used in small devices such as air-cooled condensers for the air-conditioning and automotive industry, in heat pipes, thermosyphons and other applications for system thermal control. Currently, many research centers all over the world are dealing with the structure and operation of compact refrigerating devices. This is in line with the trend of 21st century that is moving towards the use of energy-saving and environmentally friendly technical equipment. In the present study, a critical review on condensation heat transfer in microchannels and minichannels is presented. This review include a wide range of different parameters such as the channel diameter (d), the saturation temperature (T_s), the mass flux (G), the vapor quality (x), different working fluids like steam, CO_2 or R744, FC72, R22, R410A, and R407C, various shapes such as circular and noncircular, different orientations like horizontal and vertical, and systems consist of either single or multiple channels. At the end, recommendations for future studies will be given. As a result, this paper cannot only be used as the starting point for the researcher interested in condensation heat transfer in microchannels and minichannels, but it also includes recommendations for future studies on condensation heat transfer in microchannels and minichannels.
[DOI: 10.1115/1.4028092]

Keywords: critical review, condensation, heat transfer, microchannels, minichannels

1 Introduction

Condensation in microchannels and minichannels has applications in a wide variety of advanced microthermal devices. For example, condensation in microchannels and minichannels is widely used in small devices such as air-cooled condensers for the air-conditioning and automotive industry, in heat pipes, thermosyphons and other applications for system thermal control. Microchannel condensers are being used to increase heat transfer performance to reduce component size and improve energy efficiency. After 2000s, experimental data became available in open literature in condensation of various refrigerants in small hydraulic diameter microchannels.

Over the last decade, there is rapid increase in research and education on micro/nanoscale heat transfer through several dedicated individuals and teams, with direct impact now extending into other fields in both science and engineering. For example, there are many special issues on micro/nanoscale heat transfer at *ASME Journal of Heat Transfer* [1–7].

In the current review, the classification of microchannels and minichannels proposed by Kandlikar [8] is used. According to his classification, the following can be used: for microchannels, $d_h = 10$–$200\,\mu$m; for minichannels, $d_h = 200\,\mu$m–3 mm. In comparison, conventional channels have hydraulic diameters $(d_h) \geq 3$ mm. As a result, the current review covered channels have hydraulic diameters (d_h) in the range $10\,\mu\text{m} \leq d_h < 3$ mm according to the classification proposed by Kandlikar [8].

In macroscale, the gravitational forces are more important than the shear and surface tension forces, and the opposite occurs when the diameter is smaller. Also, Wang and Rose [9] cited another important influence in noncircular microchannel condensation: the viscosity in transverse flow.

2 Literature Review

Yang and Webb [10] provided heat transfer data for R12 condensation and subcooled liquid in small hydraulic diameter, flat extruded aluminum tubes. The tube outside dimensions were 16 mm × 3 mm (high) × 0.5 rrm (wall thickness). The tubes contained three internal membranes that separated the flow into four parallel channels. Two internal geometries were tested: one had a plain inner surface and the other had microfins, 0.2 mm high. The hydraulic diameter (d_h) of the plain tubes and the tubes with microfins was 2.637 and 1.564 mm, respectively. The researchers presented data for the following range of variables: mass qualities $(x) = 0.12$–0.97, mass flux $(G) = 400$–$1400\,\text{kg/(m}^2 \cdot \text{s)}$, and heat flux $(q) = 4$–$12\,\text{kW/m}^2$. They measured the overall heat transfer coefficient for water-to-refrigerant heat transfer, and used the modified Wilson plot method to determine the heat transfer coefficient for water-side flow in the annulus. Then, they extracted the tube-side condensation coefficient from the measured UA-value. Their data showed that the condensation coefficient increased with heat flux to the 0.20 power $(q^{0.2})$. The subcooled heat transfer coefficient for both the plain tubes and the tubes with microfins was well predicted using the Petukhov equation [11] with hydraulic diameter. At low mass flux, the Akers et al. correlation [12] agreed well with the plain tube data, and overpredicted the data 10–20% at high mass flux. The microfin tube showed significantly higher performance than predicted by the Akers correlation (based on hydraulic diameter) for mass quality $(x) > 0.5$. They proposed that surface tension force was effective in enhancing the condensation coefficient for mass quality $(x) > 0.5$. The proposed surface tension enhancement was particularly strong at the lower mass fluxes.

[1]Corresponding author.
Manuscript received February 15, 2014; final manuscript received July 23, 2014; published online August 25, 2014. Assoc. Editor: Calvin Li.

Webb and Zhang [13] discussed the ability of existing accepted correlations to predict single-phase and two-phase heat transfer and friction in channels of circular or rectangular shape having small hydraulic diameters (e.g., between 0.1 and 2.0 mm). The researchers showed that their recently developed "equivalent Reynolds number (Re_{eq}) model" [14] would predict the condensation coefficient of different refrigerants in tube diameters as small as 2.13 mm. However, the 1979 Shah equation [15] began to fail for R134a at $P/P_{cr} \geq 0.44$. Their study was important for applications where very small channel hydraulic diameters were important, like brazed aluminum heat exchangers or in electronic equipment cooling. Also, they mentioned that more data were needed on channel diameters below 1.0 mm.

Yan and Lin [16] investigated experimentally the characteristics of condensation heat transfer and pressure drop for refrigerant R134a flowing in a horizontal small circular pipe with an inside diameter of 2.0 mm. The researchers examined in detail the influences of the heat flux, mass flux, mass quality and saturation temperature of R134a on the measured condensation heat transfer and pressure drop. When compared with the data for a large pipe ($d_i = 8.00$ mm) reported in the literature, the condensation heat transfer coefficient averaging over the entire quality range tested here for the small pipe was about 10% higher. Also, they noted that the condensation heat transfer coefficient in the small pipe was higher at a lower heat flux, at a lower saturation temperature and at a higher mass flux. In addition, the measured pressure drop was higher for raising the mass flux but lower for raising the heat flux. Based on their data, they proposed empirical correlation equations for the condensation heat transfer coefficient and friction factors. Their correlation for the condensation heat transfer coefficient was

$$\frac{h_{tp}d}{k_l}\mathrm{Pr}_l^{-0.33}\mathrm{Bo}^{0.3}\mathrm{Re} = 6.48\mathrm{Re}_{eq}^{1.04} \tag{1}$$

$$\mathrm{Re}_{eq} = \frac{G_{eq}d}{\mu_l} \tag{2}$$

$$G_{eq} = G\left[(1-x) + x\left(\frac{\rho_l}{\rho_g}\right)^{0.5}\right] \tag{3}$$

The equivalent all liquid Reynolds number (Re_{eq}) was proposed by Akers et al. [12]. Their results were useful in designing more compact and effective condensers for different refrigeration and air-conditioning systems using refrigerant R134a.

Webb and Ermis [17] investigated the hydraulic diameter effect on single-phase and condensation heat transfer and pressure gradient for R134a in multiport flat extruded aluminum tubes. The hydraulic diameter range of the four tubes tested was between 0.44 and 1.56 mm. The researchers believed that their work provided condensation data on the smallest hydraulic diameters reported in the literature at the date of publication. They used the modified Wilson plot method to determine the heat transfer coefficient for water-side flow in the annulus. The range of mass flux was $G = 300$–$1000\ \mathrm{kg/(m^2 \cdot s)}$ while the range of mass quality (x) was approximately 15–90%. They found that the condensation coefficient and pressure gradient increased with decreasing hydraulic diameter for the four tubes. Also, they discussed the effect of hydraulic diameter on condenser design and operation. The evaluated the ability of existing correlation to predict the single-phase and condensation coefficient.

Palm [18] made an attempt to review the literature regarding heat transfer and pressure drop in one-phase and two-phase flow in microchannels. The researcher considered channels with hydraulic diameters (d_h) < 1 mm for single-phase flow. He mentioned that very little information was available for such small channels in two-phase flow. Also, deviations from large tube behavior started at diameters of a few millimeters for two-phase flow. For these reasons, he considered a slightly larger diameter range in this case. As a conclusion, it could be stated that the understanding of flow in microchannels was increasing steadily, but that there were still several questions to be answered concerning the reasons for deviations from classical theory developed for larger channels.

Zhao and Liao [19] presented an analytical model to predict film condensation of vapor flowing inside a vertical mini-equilateral triangular channel. The researchers divided the concurrent liquid–vapor two-phase flow field into three zones: the thin liquid film flow on the sidewall, the condensate flow in the corners, and the vapor core flow in the center. Their model took into account the influences of capillary force induced by the free liquid film curvature variation, interfacial shear stress, interfacial thermal resistance, gravity, axial pressure gradient, and saturation temperatures. They found that the axial variation of the cross-sectional average heat transfer coefficient of steam condensing inside an equilateral triangular channel to be substantially higher than that inside a round tube having the same hydraulic diameter, in particular in the entry region. This enhancement was attributed to the extremely thin liquid film on the sidewall, which resulted from the liquid flow toward the channel corners due to surface tension. The effects of the inlet vapor flow rates, the inlet subcooling, and the channel size on the heat transfer coefficients were also examined.

Wang et al. [20] presented the local convection heat transfer and flow regime measurements for HFC-134a condensing inside a horizontal rectangular multiport aluminum condenser tube of 1.46 mm hydraulic diameter. The researchers compared the data with condensation heat transfer correlations and flow regime maps from the literature. They found that existing correlations to over-predict both heat transfer and the stratified-to-annular flow regime transition velocity. Their experimental results suggested that liquid drawn into the corners of the tube altered the phase distribution in the annular flow regime as well as stabilizing the annular flow regime at lower vapor velocities. They developed two correlations, each representing the physics of the specific phase distributions, to predict the heat transfer data. They applied a boundary layer analysis for annular flow, in which the friction multiplier and dimensionless boundary layer temperature were evaluated specifically for this tube configuration. For stratified flow, they combined documented film condensation and single-phase forced convection correlations with straightforward void fraction weighting. Finally, they proposed successfully a weighting correlation to account for all data regardless of the mix of flow regimes experienced. This weighting applied the result of a modified flow regime map developed from the flow visualizations. Their final result was a practical correlation for the design of a condenser with millimeter-scale tubes.

Riehl et al. [21] presented an analytical model for microchannel condensers with a porous boundary, where capillary forces pumped the fluid. The researchers proposed their model as a tool to aid in the design of microchannel condensers with possible applications to microelectronics cooling, microheat exchangers, and condensers in capillary pumped loops and loop heat pipes with restricted heat dissipation area. They selected Methanol as the working fluid. They obtained very low liquid Reynolds numbers of $Re_l \sim 6$ and very high Nusselt numbers of $Nu \sim 150$ due to the channel size of 1.5 mm and the presence of the porous boundary. The meniscus calculation provided consistent results for the vapor interface temperature and pressure, as well as the meniscus curvature. They found that microchannel condensers with a porous boundary could be used for heat dissipation with reduced heat transfer area and very high heat dissipation capabilities.

Riehl and Ochterbeck [22] investigated experimentally the convective condensation heat transfer in microchannel flows. The researchers used two pumping systems in an experimental apparatus to test microchannel condensers with methanol as the working fluid. They conducted tests for two various saturation temperatures, for a range of heat dissipation rate from 20 to 350 W and four microchannel condensers. Their results showed that the

condensers presented high heat transfer capabilities with Nusselt numbers on a range of 15–600, despite the small heat transfer areas (0.0018–0.00105 m^2). They obtained an empirical correlation to calculate the Nusselt number (Nu) as a function of Weber (We), Jacob (Ja), Reynolds (Re), and Prandtl (Pr) numbers, respectively. Their correlation was

$$\mathrm{Nu} = \frac{h_m d_h}{k_l} = \mathrm{We}^{-\mathrm{Ja}}\,\mathrm{Re}_{\mathrm{Pr}}^{Y} \tag{4}$$

$$\mathrm{We} = \frac{\rho_l U^2 L}{\sigma} \tag{5}$$

$$\mathrm{Ja} = \frac{C_{p,l}\Delta T}{h_{lg}} \tag{6}$$

$$\mathrm{Re} = \frac{G d_h}{\mu_l} \tag{7}$$

$$\mathrm{Pr} = \frac{C_{p,l}\mu_l}{k_l} \tag{8}$$

$$Y = \begin{cases} 1.3 & \mathrm{Re} \le 65 \\ \dfrac{0.5 d_h - 1}{2 d_h} & \mathrm{Re} > 65 \end{cases} \tag{9}$$

They found that their correlation correlated 95% of the data within an error range of less than 25%.

Koyama et al. [23] investigated experimentally the local characteristics of pressure drop and heat transfer for the condensation of pure refrigerant R134a in two kinds of 865 mm long multiport extruded tubes having eight channels in 1.114 mm hydraulic diameter and 19 channels in 0.807 mm hydraulic diameter. The researchers measured the pressure drop at an interval of 191 mm through small pressure measuring ports. They measured the local heat transfer rate in every subsection of 75 mm in effective cooling length using heat flux sensors. They compared the data of local heat transfer coefficient with correlations of Moser et al. [14] and Haraguchi et al. [24]. The data of high mass flux agreed with the correlation of Moser et al. [14], while those of low mass flux showed different trends. The Haraguchi et al. correlation [24] showed the trend similar to the heat transfer data when the shear stress in their correlation was estimated using the Mishima and Hibiki correlation [25]. In addition, they developed their own heat transfer correlation. Their heat transfer correlation was

$$\frac{h_{tp} d}{k_l} = 0.0152(1 + 0.6\mathrm{Pr}_l^{0.8})\frac{\phi_g}{X_{tt}}\mathrm{Re}_l^{0.77} \tag{10}$$

$$X_{tt} = \left(\frac{1-x}{x}\right)^{0.9}\left(\frac{\rho_g}{\rho_l}\right)^{0.5}\left(\frac{\mu_l}{\mu_g}\right)^{0.1} \tag{11}$$

Koyama et al. [23] calculated the two-phase frictional multiplier for the gas phase in Eq. (10) using the Mishima and Hibiki correlation [25] as follows:

$$\phi_g^2 = 1 + 21[1 - \exp(-0.319 d_h)]X_{tt} + X_{tt}^2 \tag{12}$$

where d_h is in mm.

Garimella [26] presented an overview of the use of flow visualization in microchannel and minichannel geometries for the development of pressure drop and heat transfer models during condensation of refrigerants. The researcher recorded condensation flow mechanisms for round, square, and rectangular tubes with hydraulic diameters (d_h) ranging from 0.4 to 4.91 mm for mass fluxes (G) between 150 kg/($m^2 \cdot s$) and 750 kg/($m^2 \cdot s$) for $0 < x < 1$ using unique experimental techniques that permitted flow visualization during the condensation process. He documented the influence of channel shape and miniaturization on the flow regime transitions. He categorized the flow mechanisms into four various flow regimes: intermittent flow, wavy flow, annular flow, and dispersed flow. These flow regimes were further subdivided into many flow patterns within every regime. He observed that the intermittent and annular flow regimes became larger as the tube hydraulic diameter (d_h) was decreased, and at the expense of the wavy flow regime. These maps and transition lines could be used to predict the flow regime or pattern that would be established for a given mass flux (G), mass quality (x), and tube geometry. He used these observed flow mechanisms, together with pressure drop measurements, to develop experimentally validated models for pressure drop during condensation in every of these flow regimes for a variety of circular and noncircular channels with $0.4 < d_h < 5$ mm. His flow regime-based models yield substantially better pressure drop predictions than the traditionally used correlations that were primarily based on air–water flows for large diameter tubes. Also, he measured condensation heat transfer coefficients using a unique thermal amplification technique that simultaneously allowed for the accurate measurement of the low heat transfer rates over small increments of refrigerant quality and high heat transfer coefficients characteristic of microchannels. He developed models for these measured heat transfer coefficients using the documented flow mechanisms and the corresponding pressure drop models as the basis.

Shin and Kim [27] presented an experimental study of condensation heat transfer inside a minichannel with a new measurement technique. In their study, very low heat dissipation rates like several watts from the minichannel could be estimated and low mass flow rates below the 0.2 kg/h could be measured with reasonable uncertainties. To their knowledge, these techniques provided a unique experimental apparatus for measuring the condensation heat transfer coefficients inside the submillimeter hydraulic diameter single channels. By careful design and construction of the experimental apparatus, the researchers investigated experimentally the characteristics of the local heat transfer and pressure drop using the condensing R134a two-phase flow, in a horizontal single round tube, with an inner diameter of 0.691 mm. They performed tests for a mass flux of 100–600 kg/($m^2 \cdot s$), a heat flux of 5–20 kW/m^2, and a saturation temperature of 40 °C. Their experimental data of the Nusselt number and two-phase frictional pressure gradient were presented and compared with the existing correlations. Comparisons of experimental data with existing heat transfer correlations revealed that both the Shah [15] and the Akers et al. [12] correlations failed to predict the present data.

Haui and Koyama [28] investigated experimentally the local characteristics of pressure drop and heat transfer for carbon dioxide (CO_2) condensation in minichannels. The researchers used a multiport extruded aluminum test section, which had ten circular channels each with 1.31 mm inner diameter. They cooled the CO_2 with cooling water flow inside the copper blocks that were attached at both sides of the test section. They measured the temperatures at the outer surface of the test section with 24 K-type thermocouples embedded in the upper and lower surfaces along the length. They measured local heat fluxes with 12 heat flux sensors to estimate the local enthalpies, temperatures and heat transfer coefficients. They measured bulk mean temperatures of CO_2 at the inlet and outlet of the test section with 2 K-type thermocouples. They performed their measurements for the pressure (P) ranged from 6.48 to 7.3 MPa, inlet temperature (T) of CO_2 from 21.63 to 31.33 °C, heat flux (q) from 1.10 to 8.12 kW/m^2, mass flux (G) from 123.2 to 315.2 kg/($m^2 \cdot s$), and vapor quality (x) from 0 to 1. Their results indicated that pressure drop was very small along the test section, heat transfer coefficient in the two-phase region was higher than that in the single-phase, and mass flux had important influence on condensation heat transfer characteristics. Because of the large scattering of data, the influences of vapor quality on the heat transfer coefficients were not evident. Also, they compared their experimental data with previous correlations and observed large discrepancies. They concluded that the existing model failed to predict their experimental data.

Thome [29] described a state-of-the-art of heat transfer small channels (microchannels and minichannels). The researcher presented experimental methods and prediction methods for condensation inside of such small tubes, together with some comparisons of these models to selected experimental data sets and to one another.

By using unique experimental techniques and the careful construction of an experimental apparatus, Shin and Kim [30] investigated the characteristics of the local heat transfer using the condensing R134a two-phase flow in horizontal single minichannels. The researchers tested and compared the circular channels ($d = 0.493$, 0.691, and 1.067 mm) and rectangular channels (aspect ratio (AR) = 1.0 (i.e., square); $d_h = 0.494$, 0.658, and 0.972 mm). They performed tests for a mass flux (G) of 100, 200, 400, and 600 kg/(m$^2 \cdot$ s), a heat flux (q) of 5–20 kW/m^2, and a saturation temperature (T_s) of 40 °C. They investigated the effect of heat flux, mass flux, vapor qualities, hydraulic diameter, and channel geometry on flow condensation, and showed the experimental local condensation heat transfer coefficients in their study. They compared the experimental data of condensation Nusselt number with existing correlations.

The need for experimental research on condensation inside multiport minichannels came from the wide use of those channels in automotive air-conditioners. The perspective for the adoption of similar channels in the residential air-conditioning applications also called for experimental research on new high pressure refrigerants like R410A. As a result, Cavallini et al. [31] presented the experimental heat transfer coefficients measured during condensation of R134a and R410A inside multiport minichannels. Also, the researchers measured the frictional pressure gradient during adiabatic two-phase flow. They compared their experimental data against models to show the accuracy of the models in the prediction of heat transfer coefficients and pressure drop inside minichannels.

Cavallini et al. [32] reviewed published experimental work focusing on condensation flow regimes, heat transfer and pressure drop in minichannels. New experimental data were available with high pressure (R410A), medium (R134a), and low pressure (R236ea) refrigerants in minichannels of various cross section geometry and with hydraulic diameters (d_h) ranging from 0.4 to 3 mm. Because of the effect of flow regimes on heat transfer and pressure drop, the researchers presented a literature review to discuss flow regimes transitions. They compared the available experimental frictional pressure gradients and heat transfer coefficients with semi-empirical and theoretical models developed for conventional channels and with models specifically created for minichannels. Starting from their results of the comparison between experimental data and models, they discussed and evaluated the opportunity for a new heat transfer model for condensation in minichannels. Their new model attempted to take into account the influence of the entrainment rate of droplets from the liquid film.

Cavallini et al. [33] suggested a heat transfer model for condensation inside minichannels, based on analogy between heat and momentum transfer. Their proposed procedure took into account the influence of the entrainment rate of droplets from the liquid film. The researchers applied their model to the annular, annular-mist flow. Also, they presented a simplified version of the model. Comparisons between their data and predicted values showed the satisfactory behavior of both versions of the models.

Wang and Rose [34] presented a theoretical model to predict film condensation heat transfer from a vapor flowing in horizontal square and equilateral triangular section minichannels or microchannels. Their model was based on fundamental analysis that assumed laminar condensate flow on the channel walls and took account of surface tension, interfacial shear stress, and gravity. The Wang and Rose [34] theory was based on the Nusselt [35] assumptions but included the streamwise shear stress on the condensate film surface and, most importantly, the transverse pressure gradient due to surface tension in the presence of curvature of the condensate surface. Results are given for channel sizes (side of square or triangle) in the range of 0.5–5 mm and for refrigerants R134a, R22, and R410A. The researchers considered that the channel wall temperature was uniform and the vapor was saturated at the inlet. They found that the general behavior of the condensate flow pattern (spanwise and streamwise profiles of the condensate film), as well as streamwise variation of local mean (over section perimeter) heat transfer coefficient and vapor mass quality, were qualitatively in accord with expectations on physical grounds. The magnitudes of the calculated heat transfer coefficients agreed in general with experimental data for similar, but nonidentical, channel geometry, and flow parameters.

Bandhauer et al. [36] presented a model for predicting heat transfer during condensation of refrigerant R134a in horizontal microchannels. The researchers used the thermal amplification technique to measure condensation heat transfer coefficients accurately over small increments of refrigerant quality across the vapor–liquid dome ($0 < x < 1$). A combination of a high flow rate closed-loop primary coolant and a low flow rate open-loop secondary coolant ensured the accurate measurement of the small heat duties in these microchannels and the deduction of condensation heat transfer coefficients from measured UA values. They conducted measurements for three circular microchannels ($0.506 < d_h < 1.524$ mm) over the mass flux range $150 < G < 750$ kg/(m$^2 \cdot$ s). They used the results from their previous work on condensation flow mechanisms in microchannel [26] geometries to interpret the results based on the applicable flow regimes. They based their heat transfer model on the approach originally developed by Traviss et al. [37] and Moser et al. [14]. They used the multiple-flow-regime model of Garimella et al. [38] to predict the pertinent interfacial shear stresses required in their heat transfer model. They found that their resulting heat transfer model predicted 86% of the data within ±20%.

Cavallini et al. [39] presented the first preliminary tests carried on a new experimental rig for measurement of the local heat transfer coefficient inside a circular 0.8 mm diameter minichannel. The researchers measured the heat transfer coefficient during condensation of R134a and obtained from the measurement of the heat flux and the direct gauge of the saturation and wall temperatures. They derived the heat flux from the water temperature profile along the channel to get local values for the heat transfer coefficient. They designed the test section so as to reduce thermal disturbances and experimental uncertainty. They reported a brief insight into the design and the construction of the test rig. The apparatus was designed for experimental tests both in condensation and vaporization, in a wide range of operating conditions and for a wide selection of refrigerants.

The phenomenon of two-phase flow and heat transfer mechanism in small diameter microchannels (<1 mm) might be different than that in conventional tube sizes due to increasing dominance of many affecting parameters such as surface tension, viscosity, etc. As a result, Chowdhury et al. [40] presented an on-going experimental study of condensation heat transfer and pressure drop of refrigerant R134a was a single high AR rectangular microchannel of hydraulic diameter (d_h) = 0.7 mm and AR = 7. Their data would help explore the condensation phenomenon in microchannels that was necessary in the design and development of small-scale heat exchangers and other compact cooling systems. In their study, they used the range of the inlet vapor qualities (x_i) was between 20% and 80% and mass fluxes (G) of 130 and 200 kg/m$^2 \cdot$ s. They maintained the microchannel outlet conditions at close to thermodynamic saturated liquid state through a careful experimental procedure. They adopted a unique process for fabrication of the microchannel involving milling and electroplating steps to maintain the channel geometry close to design values. Measurement instruments were well-calibrated to ensure low system energy balance error, uncertainty and good repeatability of test data. They compared the trends of data recorded to that found in recent literature on similar dimension tubes.

Wang and Rose [41] presented a progress report on a theoretical study of film condensation in microchannels. Their model took

account of surface tension, vapor shear stress and gravity. The researchers investigated the effect of channel shape for condensation of R134a in channels with cross sections: square, triangle, inverted triangle, rectangle with longer side vertical, rectangle with longer side horizontal, and circle. They considered the case where the channel wall temperature was uniform and the vapor was saturated at inlet. For a given mass flux, they calculated the local condensate film profile around the cross section together with the mean heat transfer coefficient at various distances along the channel. They presented results for one vapor mass flux, one vapor temperature, and one wall temperature.

Garimella [42] reviewed a large number of the existing studies on minichannel to microchannel condensation covering the flow pattern, void fraction, pressure drop, and heat transfer prediction methods. The researcher presented the available relevant information on heat transfer coefficients in condensing flows through relatively small channels and primarily adiabatic flows through microchannels in tabular form. Also, he compared different techniques for predicting the heat transfer coefficients during condensation of refrigerant R134a flowing through a 1 mm diameter tube, at a mass flux of 300 $\mathrm{kg/(m^2 \cdot s)}$, at a mean quality of 0.5 and a pressure of 1500 kPa. He showed graphically a comparison of the heat transfer coefficients predicted by these different techniques. He found that the predicted heat transfer coefficients varied considerably, from 3216 to 4703 $\mathrm{W/m^2 \cdot K}$. He attributed these considerable variations between the heat transfer coefficients predicted by these different models and correlations to most of these correlations were applied in this case outside their ranges of applicability, either in the mass flux, the phase velocities, or parameters like the Weber and Froude numbers as applicable. But the most important reason for the differences was that all except the Bandhauer et al. [36] model were based primarily on tube diameters in the ~8 mm range, with a few correlations being proposed based on limited data on ~3 mm tubes. The channel under consideration in his example was a 1-mm channel.

Jokar et al. [43] investigated the parameters that affected the two-phase heat transfer within the minichannel plate heat exchangers, and utilized the dimensional analysis technique to develop appropriate correlations. For this purpose, the researchers analyzed experimentally thermohydrodynamic performance of three minichannel brazed-type plate heat exchangers in their study. They used these heat exchangers as the evaporator and condenser of an automotive refrigeration system where the refrigerant R134a flowed on one side and a 50% glycol–water mixture on the other side in a counter-flow configuration. First, they obtained the heat transfer coefficient for the single-phase flow of the glycol–water mixture using a modified Wilson plot technique. Then, they used the results from the single-phase flow analysis in the two-phase flow analysis, and developed correlations for the refrigerant evaporation and condensation heat transfer. Also, they obtained correlations for the single-phase and two-phase Fanning friction factors based on a homogenous model. Their results showed that the two-phase theories and correlations that were established for conventional macrochannel heat exchangers might not hold for the minichannel heat exchangers used in their study.

Dessiatoun et al. [44] analyzed three different refrigerants, R134a, R245fa, and HFE7100 as working fluids for two-phase cooling of high heat flux electronics in a 0.7 mm hydraulic diameter 190 mm long high AR minichannel and in a newly developed microgroove surface condenser. The latter comprised of a microgroove surface with rectangular grooves of 84 μm in hydraulic diameter with an AR of 10.6 and headers, which directed the refrigerant flow into the grooves. The researchers concluded that R245fa provided higher heat transfer coefficients compared to R134a with a significantly higher pressure drop in the minichannel. The saturation temperature drop in the same channel created a significant temperature drop for HFE7100, which made the application of such minichannels for cross-flow condensers with this fluid unpractical. The microgroove surface condenser provided significantly higher heat transfer coefficients compared to the minichannel condenser. The pressure drop in the microgroove surface condenser was extremely low and imposed just 1 °C temperature drop on HFE7100 at its highest heat flux. The mass flux of refrigerant in the microgroove surface condenser was significantly lower compared to conventional minichannel and microchannel condensers. In this configuration, the microgroove surface condenser benefited from the possibility of an increase in mass flux resulting in a significant increase in heat transfer coefficient and just a moderate increase in pressure drop.

Chen et al. [45] discussed and evaluated recent investigations of condensation heat transfer in microchannels. The researchers presented a review of both experimental and theoretical analyses of condensation in the microchannels, with special attention given to the influences of channel diameter and surface conditions on the flow regimes of condensing flows occurring in these channels. Their review suggested that surface tension, rather than body or buoyancy forces, was the dominant force that governed the condensation and two-phase flow in these microchannels. Recent experimental results indicated that with decreases in the channel diameter, the dominant condensing flow pattern is intermittent injection/slug/bubble flow, as opposed to stratified or annular flow, which is typically found in two-phase flows in larger 1g channel flows. As a result, existing annular flow condensation models cannot be used to accurately represent or predict the actual physical mechanisms that occur in these condensing flows in microchannels. This therefore necessitates the use of semi-theoretical models or correlations based upon experimental data. Since wettability and surface roughness play an important role in the condensing flow in microchannels, an optimization of these effects may provide a mechanism by which very high condensation heat fluxes can be achieved.

Cheng et al. [46] reviewed recent work on boiling of water and condensation of steam in single and parallel microchannels in their study. The researchers investigated transition from annular flow to slug/bubbly flow for condensation in a microchannel. The occurrence of the injection flow was owing to the instability of the liquid/vapor interface. The location, at which the injection flow occurs, was dependent on the mass flux and the cooling rate of steam. Increase in steam mass flux, decrease in cooling rate, and microchannel diameter tended to enhance the condensate film instability on the wall, resulting in the occurrence of injection flow further downstream at increasingly high frequency. The pressure drop in the condensing flow increased with the increase in mass flux (G) and mass quality (x) or with decreasing microchannel diameter (d). The existing correlations for pressure drop and heat transfer of condensing flow in macrochannels overestimated the experimental data in microchannels.

Matkovic et al. [47] reported local heat transfer coefficients obtained from the measurement of the local heat flux and the direct measurement of the saturation and wall temperatures during condensation of R134a and R32 within a single circular 0.96 mm diameter minichannel. Except for the lowest mass flux, the researchers did not find significant discrepancy from the trends expected for macroscale tubes.

Park and Hrnjak [48] investigated the CO_2 flow condensation heat transfer coefficients and pressure drop in multiport microchannels made of aluminum having a hydraulic diameter (d_h) of 0.89 mm at low temperatures in horizontal flow conditions. The researchers performed their measurements at saturation temperatures (T_s) of −15 and −25 °C, mass fluxes (G) from 200 to 800 $\mathrm{kg/(m^2 \cdot s)}$, and wall subcooling temperatures from 2 to 4 °C. Before investigating heat transfer and pressure drop, they predicted the flow patterns for experimental conditions using the Akbar et al. [49] and the Breber et al. [50] flow pattern maps. These flow pattern maps demonstrated that the flow patterns were annular flow patterns in most of flow conditions, and intermittent flow patterns could occur at low and medium vapor qualities for the mass fluxes of 200 $\mathrm{kg/(m^2 \cdot s)}$. They found that measured heat transfer coefficients increased with the increase of mass fluxes and vapor qualities, whereas measured heat transfer coefficients

were almost independent of wall subcooling temperature changes. Many correlations could predict the heat transfer coefficients within acceptable error range such as the Thome et al. [51] model, and from this comparison, it could be inferred that the flow condensation mechanism in 0.89 mm channels should be similar to that in large tubes.

Su et al. [52] reviewed earlier experimental work of the heat transfer coefficients during condensation in microchannels. The researchers compared a wholly theoretical model with the correlations for both R134a and ammonia (NH_3). They drew attention, to the fact that, while four various correlations for condensation in microchannels were in fair agreement for the case of R134a (on which the empirical constants in the correlations were predominately based) they differed markedly when applied to other fluids like ammonia. The prediction for ammonia relative to those of the correlations was dependent on the vapor mass flux. Apart from suggesting that heat transfer coefficient for ammonia might be around ten times those for R134a under similar conditions, all that could be said from those comparisons was that it would be unsafe to use any of the correlations for fluids with properties widely different from those on that they were based. The general validity of the theory must await further and more accurate data for a range of fluids.

Matkovic et al. [53] presented experimental heat transfer coefficients measured during condensation inside a single square cross section minichannel, having a 1.18 mm side length. The researchers compared the experimental heat transfer coefficients to the ones previously obtained in a circular minitube [47]. This subject was particularly interesting because most of the minichannel and microchannels used in practical applications had noncircular cross sections. They obtained the test section used in this work from a thick wall copper tube that was machined to draw a complex passage for the water. They studied its geometry with the aim of increasing the external heat transfer area and thus decreasing the external heat transfer resistance. This experimental technique allowed to measure directly the temperature in the tube wall and in the water channel. The determined the heat flux from the temperature profile of the coolant in the measuring sector. They measured the wall temperature by means of thermocouples embedded in the copper tube, while obtained the saturation temperature from the saturation pressure measured at the inlet and outlet of the measuring sector. On the whole, they placed more than seventy thermocouples in the 23 cm long measuring section. They performed tests with R134a as the working fluid at saturation temperature (T_s) of 40 °C, at mass flux (G) ranging between 200 and 800 kg/(m$^2\cdot$s). As compared to the heat transfer coefficients measured in a circular minichannel, they found a heat transfer enhancement in the square minichannel at the lowest values of mass flux. This must be due to the surface tension effect. Also, they found no heat transfer coefficient increase at the highest values of the mass flux where condensation was shear stress dominated.

In his Ph.D. thesis, Marak [54] investigated condensation heat transfer and pressure drop for methane (CH_4) and binary methane fluids in small channels. The researcher used an experimental setup designed by Dr. Steffen Grohmann in these investigations. He did a total of 749 measurements in tubes with diameter 1 mm, 0.5 mm, and 0.25 mm. He carried out both single and two-phase flow measurements of pure CH_4, methane/ethane- and methane/nitrogen mixtures. The measurements were done over a broad range with respect to pressure, mass fraction, mass flux, and heat flux. Also, the pressure drop was measured. He found that the models concerning heat transfer and pressure drop in conventional channels also could be used in tubes with diameter 1 mm and 0.5 mm while the results from the 0.25 mm tube were burdened with too high uncertainty to be used. In addition, the results could be relevant for noncircular diameters in microscale, e.g., for plate-fin heat exchangers.

Huang et al. [55] investigated experimentally the oil effect on condensation heat transfer of R410A inside 4.18 mm and 1.6 mm inner diameter horizontal smooth tubes. The experimental condensing temperature was 40 °C, and nominal oil concentration range was from 0% to 5%. Their test results indicated that the presence of oil deteriorated the heat transfer, and the deterioration influence became clear with the increase of oil concentration. At oil concentration of 5%, the heat transfer coefficient decreased by maximum 24.9% and 28.5% for 4.18 mm and 1.6 mm tubes, respectively. The researchers proposed a new correlation for heat transfer coefficients of R410A-oil mixture flow condensation inside smooth tubes. Their correlation was

$$\frac{h_{tp}d}{k_l} = 0.0152(-0.33 + 0.83\mathrm{Pr}_l^{0.8})\frac{\phi_g}{X_{tt}}\mathrm{Re}_l^{0.77} \tag{13}$$

$$X_{tt} = \left(\frac{1-x}{x}\right)^{0.9}\left(\frac{\rho_g}{\rho_l}\right)^{0.5}\left(\frac{\mu_l}{\mu_g}\right)^{0.1} \tag{14}$$

Huang et al. [55] calculated the two-phase frictional multiplier for the gas phase in Eq. (13) by using the Haraguchi et al. [24] correlation as follows:

$$\phi_g = 1 + 0.5\left[\frac{G}{\sqrt{g\rho_g(\rho_l-\rho_g)d}}\right]X_{tt}^{0.35} \tag{15}$$

They found that their correlation agreed with all the experimental data within a deviation of −30% to +20%. We can notice that Huang et al. [55] correlation, Eq. (13), is very similar to Koyama et al. [23] correlation, Eq. (10), except at:

(i) The term $(1+0.6\mathrm{Pr}_l^{0.8})$ in Eq. (10) becomes $(-0.33+0.83\mathrm{Pr}_l^{0.8})$ in Eq. (13).
(ii) ϕ_g is calculated in Eq. (10) using the Mishima and Hibiki correlation [25] while ϕ_g is calculated in Eq. (13) using the Haraguchi correlation [24].

Agarwal and Garimella [56] measured condensation pressure drops and heat transfer coefficients for refrigerant R134a flowing through rectangular microchannels with hydraulic diameters (d_h) ranging from 100 μm to 200 μm in small quality increments. These microchannels were fabricated on a copper substrate by electroforming copper onto a mask patterned by X-ray lithography and sealed by diffusion bonding. The researchers heated electrically subcooled liquid to the desired quality, followed by condensation in the test section. Downstream of the test section, they used another electric heater to heat the refrigerant to a superheated state. Energy balances on the preheaters and postheaters established the refrigerant inlet and outlet states at the test section. Water at a high flow rate served as the test-section coolant to ensure that the condensation side presented the governing thermal resistance. They measured heat transfer coefficients for mass fluxes (G) ranging from 200 kg/(m$^2\cdot$s) to 800 kg/(m$^2\cdot$s) for $0 <$ mass quality (x) < 1 at many various saturation temperatures. They conducted conjugate heat transfer analyses in conjunction with local pressure drop profiles to obtain accurate driving temperature differences and heat transfer coefficients. They illustrated the influences of mass quality, mass flux, and saturation temperature on condensation pressure drops and heat transfer coefficients through their experiments.

Song et al. [57] reported preliminary results from a new research program for making accurate heat transfer and pressure drop measurements during condensation in microchannels. While commissioning the apparatus, the researchers used a dummy test section with identical channel and header geometry to that to be used in the main test program (The final test section would comprise a relatively thick copper test section containing 98 accurately located thermocouples for measuring the temperature distribution from which local heat flux and temperature at the microchannel surface would be obtained). While using the dummy test section (without embedded thermocouples), they took

the opportunity to make accurate pressure drop measurements while measuring the vapor flow rate and total heat transfer rate based on coolant measurements. They obtained data for FC72 and steam. Also, they presented approximate comparisons with available pressure drop calculation methods.

Keinath and Garimella [58] investigated condensation of Refrigerant R404a in channels of diameter 0.5–3 mm. The researchers obtained quantitative information on flow mechanisms using image analysis techniques on high speed video. They conducted experiments on condensing R404a at mass fluxes (G) ranging from 200 to 800 kg/(m^2 · s) at vapor qualities (x) of 0.05–0.95. They conducted the experiments at the high pressures representative of actual operation of air-conditioning and refrigeration equipment, instead of extrapolating findings for adiabatic air–water mixtures at atmospheric pressure to high pressure refrigerant condensation. Also, they measured pressure drops as a function of geometry and operating conditions during the flow visualization experiments. Quantitative image analysis enabled detailed computation of void fraction and vapor bubble parameters like frequency, velocity, diameter, and length with a high degree of repeatability and with low uncertainties. They documented the operating conditions effect on the flow patterns, void fractions, and vapor bubble parameters for saturation temperatures ranging from 30 to 60 °C. The resulting void fraction models provided closure for pressure drop and heat transfer models that had thus far not been possible in the reported works in the literature.

Fronk and Garimella [59] measured heat transfer coefficients and pressure drops during condensation of CO_2 in small quality increments in microchannels of $100 < d_h < 200\ \mu$m. These microchannels were fabricated on a copper substrate by electroforming copper onto a mask patterned by X-ray lithography, and sealed by diffusion bonding. The researchers cooled the test section using chilled water circulating at a high flow rate in order to ensure that the thermal resistance on the condensation heat transfer side dominated. A conjugate heat transfer analysis in conjunction with local pressure drop profiles allowed driving temperature differences, heat transfer rates, and condensation heat transfer coefficients to be determined accurately. They measured heat transfer coefficients for mass flux (G) = 600 kg/(m^2 · s) for 0 < mass quality (x) < 1 and multiple saturation temperatures. They presented preliminary results for a $300 \times 100\ \mu$m (15 channels) test section. They used these data in order to evaluate the applicability of correlations developed for larger hydraulic diameters and various fluids for predicting condensation heat transfer and pressure drop of CO_2.

Agarwal et al. [60] measured in their study heat transfer coefficients in six noncircular horizontal microchannels ($0.424 < d_h < 0.839$ mm) of various shapes during condensation of refrigerant R134a over the mass flux range $150 < G < 750$ kg/(m^2 · s). The noncircular microchannels included barrel-shaped, N-shaped, rectangular, square, and triangular extruded tubes, and a channel with a W-shaped corrugated insert that yielded triangular microchannels. They used the thermal amplification technique developed and reported in their earlier work to measure the heat transfer coefficients across the vapor–liquid dome in small increments of vapor quality. They used results from their previous work on condensation flow mechanisms in microchannel geometries to interpret the results based on the applicable flow regimes. Also, they considered the influence of tube shape in deciding the applicable flow regime. They found that a modified version of the annular-flow-based heat transfer model proposed recently by the authors for circular microchannels [36], with the required shear stress being calculated from a noncircular microchannel pressure drop model [61] also reported earlier to best correlate their data for square, rectangular and barrel-shaped microchannels. For the other microchannel shapes with sharp acute-angle corners, they found that a mist-flow-based model proposed by Soliman [62] on larger tubes to suffice for the prediction of the heat transfer data. Their models predicted the data significantly better than the other available correlations in the literature.

Del Col et al. [63] reported local heat transfer coefficients measured during condensation of R1234yf within a single circular 0.96 mm diameter minichannel and compared them to the ones of R134a. The researchers carried out their experimental work in a unique test apparatus that allowed to determine the local heat flux extracted from the condensing fluid from the temperature profile of the coolant. For this purpose, they measured the temperatures of the coolant and of the wall along the test section. They determined the saturation temperature from the saturation pressure that was measured at inlet and outlet of the test channel. They carried out condensation tests at mass fluxes (G) ranging between 200 and 1000 kg/(m^2 · s) and the heat transfer coefficients result to be lower as compared to the ones of R134a. Since the saturation temperature drop had direct effects on the heat transfer rate, they measured and compared also the pressure drop during adiabatic two-phase flow of R1234yf to R134a.

Kuo and Pan [64] investigated experimentally steam condensation in rectangular microchannels with uniform and converging cross sections and a mean hydraulic diameter (d_h) of 135 μm. The researchers cooled the steam flow in the microchannels using water cross-flowing along its bottom surface that was different from other methods reported in the literature. They determined the flow patterns, two-phase flow pressure drop and condensation heat transfer coefficient. They found that the microchannels with the uniform cross section design had a higher heat transfer coefficient than those with the converging cross section under condensation in the mist/annular flow regimes, although the latter worked best for draining two-phase fluids composed of uncondensed steam and liquid water, which was consistent with the result of their previous study [65]. Using their experimental results, they developed dimensionless correlations of condensation heat transfer for the mist and annular flow regions and a two-phase frictional multiplier for the microchannels with both types of cross section designs. Their experimental data agreed well with the obtained correlations, with the maximum mean absolute errors (MAEs) of 6.4% for the two-phase frictional multiplier and 6.0% for the condensation heat transfer.

In his Ph.D. thesis, Bortolin [66] studied two-phase heat transfer inside minichannels. The researcher measured the local heat transfer coefficients in circular and rectangular horizontal single microchannels made of copper during condensation of refrigerants R245fa, and R134a. The used hydraulic diameter (d_h) was 0.96 and 1.23 mm. The range of mass flux was G = 67–789 kg/(m^2 · s).

Cavallini et al. [67] presented experimental data for heat transfer and pressure drop during condensation of the refrigerants R32 and R245fa in a single circular minichannel of d = 0.96 mm. The researchers performed their experiments at saturation temperature (T_s) around 40 °C, corresponding to 24.8 bar saturation pressure for R32 and 2.5 bar saturation pressure for R245fa. They performed the pressure drop tests have in adiabatic flow conditions to measure only the pressure losses due to friction. They compared their heat transfer experimental data against predicting models to provide a guideline for the design of minichannel condensers. The experimental values of the heat transfer coefficient showed that the condensation was shear stress dominated for most of the data points, and in this range of operating conditions they could be well predicted by using the Cavallini et al. [68] model for macroscale condensation.

Goss et al. [69] investigated experimentally the pressure drop and local heat transfer coefficient during the convective condensation of R134a inside eight round (d = 0.8 mm) horizontal and parallel microchannels over a mass flux range of $57 < G < 125$ kg/(m^2 · s) and pressure range of $6.8 < P < 11.2$ bar. The researchers compared their experimental results with correlations and semi-empirical models described in the literature. For the heat transfer coefficient, the Yan and Lin [16] correlation gave the best results compared with the experimental data. For $x < 0.9$ (intermittent region on the Coleman and Garimella [70] map) this correlation fitted the experimental data very well, with a mean deviation of 13%.

Park et al. [71] presented and compared experimental condensation heat transfer data for the new refrigerant R1234ze(E), trans-1,3,3,3-tetrafluoropropene, with refrigerants R134a and R236fa for a vertically aligned, aluminum multiport tube. Local condensation heat transfer measurements with such a multimicrochannel test section were very challenging because of the large uncertainties related to the heat flux estimation. Therefore, the researchers designed a new experimental test facility with a test section to directly measure the wall temperature along a vertically aligned aluminum multiport tube with rectangular channels of 1.45 mm hydraulic diameter. Then, they developed a new data reduction process to compute the local condensation heat transfer coefficients accounting for the nonuniform distribution of the local heat flux along the channels. The condensation heat transfer coefficients showed the expected decrease as the mass quality (x) decreased (1.0–0.0) during the condensation process, as the mass flux (G) decreased (260–50) kg/(m$^2 \cdot$ s) and as the saturation temperature (T_s) increased (25–70 °C). However, the heat transfer coefficients were not affected by the condensing heat flux (q) (1–62 kW/m^2) or by the entrance conditions within the tested range. They found that the heat transfer performance of R1234ze(E) was about 15–25% lower than for R134a but relatively similar to R236fa. Then, they compared the experimental data with leading prediction methods from the literature for horizontal channels. In general, the agreement was poor, overpredicting the high Nusselt number data and underpredicting the low Nusselt number data, but capturing the midrange quite well. As a result, they developed a modified correlation. Their correlation was

$$\frac{h_{tp} d_h}{k_l} = 0.0055 \mathrm{Pr}_l^{1.37} \frac{\phi_g}{X_{tt}} \mathrm{Re}_l^{0.7} \tag{16}$$

$$X_{tt} = \left(\frac{1-x}{x}\right)^{0.9} \left(\frac{\rho_g}{\rho_l}\right)^{0.5} \left(\frac{\mu_l}{\mu_g}\right)^{0.1} \tag{17}$$

Park et al. [71] calculated the two-phase frictional multiplier for the gas phase in Eq. (16) as follows:

$$\phi_g^2 = 1 + 13.17 \left(\frac{\rho_g}{\rho_l}\right)^{0.17} \left[1 - \exp\left(-0.6 \sqrt{\frac{g(\rho_l - \rho_g) d_h^2}{\sigma}}\right)\right] X_{tt} + X_{tt}^2 \tag{18}$$

They found that their correlation yielded a good agreement with their database for all three fluids over a wide range of operating conditions.

Oh and Son [72] investigated experimentally the condensation heat transfer coefficients of R22, R134a, and R410 A in a single circular microtube. The researchers conducted their experiments without oil in the refrigerant loop. The test section was a smooth, horizontal copper tube of 1.77 mm inner diameter. They conducted their experiments at mass flux of 450–1050 kg/(m$^2 \cdot$ s), saturation temperature of 40 °C. The test results showed that in case of single-phase flow, the single-phase Nusselt Number measured by experimental data was higher than that calculated by Gnielinski correlation [73]. In case of two-phase flow, the condensation heat transfer coefficient of R410 A was higher than that of R22 and R134a at the given mass flux. The condensation heat transfer coefficient of R22 showed almost a similar value to that of R134a. Most of the existing correlations that were proposed in the large diameter tube failed to predict condensing heat transfer. And also, recently proposed correlation in the single circular microtube is considered not adequate for small diameter tube. Therefore, it is necessary to develop accurate and reliable correlation to predict heat transfer characteristics in the single circular microtube.

Bohdal et al. [74] presented the results of experimental investigations of heat transfer and pressure drop during the condensation of the R134a and R404A refrigerants in pipe minichannels with internal diameters (d_i) = 0.31–3.30 mm. Their results concerned investigations of the local heat transfer coefficient and a pressure drop in single minichannels. Within the range of the examined parameters of the condensation process in minichannels produced from stainless steel, the researchers found that the values of the local heat transfer coefficient and the pressure drop in the above mentioned minichannels were higher for R134a than R404A. Also, they compared their results with calculations according to the correlations proposed by other authors. Within the range of the examined parameters of the condensation process in minichannels produced from stainless steel, they showed that the values of the heat transfer coefficient might be described with Akers et al. [12] and Shah [15] correlations within a limited range of the mass flux density of the refrigerant and the minichannel diameter. On the basis of their experimental investigations, they proposed their own correlation for the calculation of local heat transfer coefficient. Their correlation was

$$\frac{h_{tp} d}{k_l} = 25.084 \mathrm{Re}_l^{0.258} \mathrm{Pr}_l^{-0.495} \left(\frac{P}{P_{cr}}\right)^{-0.288} \left(\frac{x}{1-x}\right)^{0.266} \tag{19}$$

Wang and Rose [9] presented a theoretical model for condensation in microchannels with taking account of the influences of gravity and streamwise shear stress on the condensate surface as well as the transverse pressure gradient due to surface tension in the presence of change in condensate surface curvature. The researchers updated their original theory [34] and incorporated new results. In particular, attention was drawn to the fact that there existed conditions under which gravity, shear stress and position along the channel had minor effect on the heat transfer coefficient (for uniform vapor-to-surface temperature difference). Here the problem was governed by a balance between surface tension and viscosity in transverse flow. They obtained numerical solutions of the relevant conservation equations for different channel shapes, dimensions, vapor-to-surface temperature differences and vapor mass fluxes. They reviewed and updated the theory. They included the channel inclination influence and presented new results. When using boundary conditions of uniform vapor and surface temperature, they found that, over a certain length of channel, the local mean (around the channel perimeter) heat transfer coefficient was essentially independent of gravity and vapor shear stress. For the surface tension dominated regime, they derived an equation for the Nusselt number as a function of a single dimensionless group, analogous to that occurring in the simple Nusselt theory except that the gravity term was replaced by a surface tension term, both on the basis of dimensional analysis and by approximate theory. Their equation represented all of the data satisfactorily. This was a step towards the goal of representing the solutions, including those conditions where shear stress and gravity played important roles, by relatively simple dimensionless algebraic equations, valid for any fluid and channel geometry, for convenient use in design and optimization.

Guermit [75] presented a simulation study of the condensation inside a minitube. The researcher developed the physical model and considered the condensation of pure refrigerants and binary mixtures. He used R407d (R32/R125/R134a) (5/2015/80). In his study, he did not take into account the condensation of R32 because its concentration was negligible compared to other refrigerants. His study covered the effect of many parameters on condensation, the concentration of the mixture, the vapor velocity, the diameter of the tube condensation. He found that the heat transfer was enhanced by reducing the diameter of the minitube. Also, he made a comparison between the results from his numerical model and those determined from the correlations.

Alshqirate et al. [76] obtained the experimental results of the convection heat transfer coefficient and pressure drop values during condensation and evaporation of CO_2 at various operating conditions for flow inside micropipes of 0.6, 1.0, and 1.6 mm

internal diameter. The range of Reynolds number (Re_d) was between 2000 and 15,000. The researchers utilized the dimensional analysis technique to develop correlations for Nusselt numbers and pressure drops. For the pressure drops, they assumed that the pressure drop of any gas during condensation (ΔP_{cond}) was dependent on the following dimensional variables: micropipe condenser inlet pressure ($P_{in,cond}$); the micropipe internal diameter (d_i); the length of the micropipe condenser (L); the mean velocity (V_m); and the mean value of the density (ρ_m) and the dynamic viscosity (μ_m). They obtained a general formula for the average Nusselt number (Nu_{av}) during condensation. Solving for CO_2 data generated by their experimental work using the Multiple Linear Regression Method would give the following correlation:

$$Nu_{av} = \frac{h_{tp} d_i}{k_m} = 34.92 * \left[(Re_d)^{-0.31} (Pr)^{-0.39} (Ga)^{0.11} (Ja)^{-0.71} \times (We)^{0.81} \left(\frac{L}{d_i} \right)^{-0.82} (Eu)^{0.2} \right] \quad (20)$$

$$Re_d = \frac{\rho_m d_i U_m}{\mu_m} \quad (21)$$

$$Pr = \frac{C_{p,m} \mu_m}{k_m} \quad (22)$$

$$Ga = \frac{g(\rho_l - \rho_g) d_i^3 \rho_m}{\mu_m^2} \quad (23)$$

$$Ja = \frac{C_{p,m} \Delta T}{h_{lg}} \quad (24)$$

$$We = \frac{\rho_m U_m^2 d_i}{\sigma} \quad (25)$$

$$Eu = \frac{P_{in,cond}}{U_m^2 \rho_m} \quad (26)$$

It should be noted that the mean values of the properties were defined by liquid and gas properties. For example

$$\rho_m = \frac{\rho_l + \rho_g}{2} \quad (27)$$

$$\mu_m = \frac{\mu_l + \mu_g}{2} \quad (28)$$

They carried out a comparison between experimental and correlated results. The results showed that for the condensation process, the bias errors were 5.25% and 0.4% for pressure drops and Nusselt number, respectively. Consequently, average standard deviation (ASD) values reached 17.94% and 4.62% for both, respectively. On the other hand, for the evaporation process, the Nusselt number error was 3.8% with an ASD of 4.14%. Their correlations could be used in calculating pressure drops and heat transfer coefficients for phase change flows in mini- and microtubes. Also, their correlations could help to enhance design calculations of heat exchangers, condensers and evaporators.

Derby et al. [77] measured condensation heat transfer coefficients in square, triangular and semicircular minichannels with smaller measurement uncertainties than previously obtained using three specially designed copper test sections. Single-phase experiments validated the approach. The researchers reported data for R134a in 1 mm square, triangular, and semicircular multiple parallel minichannels cooled on three sides. They conducted a parametric study over a range of conditions for mass flux, average quality, saturation pressure, and heat flux. They found that mass flux and quality had significant effects on the condensation process, even at lower mass fluxes, while saturation pressure, heat flux, and channel shape had no significant effects. They attributed the lack of shape effects to the three-sided cooling boundary conditions. Because there was no significant surface tension enhancement, the macroscale Shah [78] correlation best predicted their data, with a mean average error (MAE) of 20–30% for all geometries.

Kim and Mudawar [79] examined the pressure drop and heat transfer characteristics of annular condensation in rectangular microchannels with three-sided cooling walls. The researchers proposed a theoretical control-volume-based model based on the assumptions of smooth interface between the annular liquid film and vapor core, and uniform film thickness around the channel's circumference. They applied mass and momentum conservation to control volumes encompassing the liquid film and the vapor core separately. Their model took into account for interfacial suppression of turbulent eddies due to surface tension with the aid of a new eddy diffusivity model specifically tailored to shear-driven turbulent films. They compared their model predictions with experimental pressure drop and heat transfer data for annular condensation of FC72 along 1×1 mm^2 parallel channels. They achieved the condensation by rejecting heat to a counter flow of water. The data spanned FC72 mass fluxes (G) of 248–367 kg/(m$^2 \cdot$ s), saturation temperatures (T_s) of 57.8–62.3 °C, mass qualities (x) of 0.23–1.0, and water mass flow rates of 3–6 g/s. Also, they compared the data to predictions of previous separated flow mini/microchannel and macrochannel correlations. While some of the previous correlations did provide good predictions of the average heat transfer coefficient, they failed to capture axial variation of the local heat transfer coefficient along the channel. Their new model accurately captured the pressure drop and heat transfer coefficient data in both magnitude and trend, evidenced by MAE values of 3.6% and 9.3%, respectively.

In order to continue the first part of their study on flow condensation in parallel microchannels, which was related to experimental results and assessment of pressure drop correlations [80], Kim and Mudawar [81] presented in their second part of a two-part study the heat transfer characteristics for FC72 condensing along parallel, square microchannels with a hydraulic diameter (d_h) of 1 mm that were formed in the top surface of a solid copper plate. Heat from the condensing flow was rejected to a counter flow of water through channels brazed to the underside of the copper plate. The FC72 condensation heat transfer coefficient was highest near the channel inlet, where the annular liquid film was thinnest. The heat transfer coefficient decreased along the microchannel because of the film thickening and eventual collapse of the annular regime. They observed notable heat transfer enhancement for annular flow regions of the microchannel associated with interfacial waves. Comparing their present data to predictions of previous annular condensation heat transfer correlations showed correlations intended for macrochannels generally provide better predictions than correlations intended specifically for mini/microchannels. They proposed a new condensation heat transfer coefficient correlation for annular condensation heat transfer in mini/microchannels. The local heat transfer coefficient for annular condensation with three-sided cooling can be expressed as follows:

$$h_{tp} = \left(\frac{Nu_3}{Nu_4} \right) (0.1 + 0.06 Pr_l^{0.8}) Pr_l^{-1} Re_l^{-0.13} Cp_l \times \sqrt{\frac{fG^2(1-x)^2}{2} \left\{ 1 + \frac{21[1 - \exp(0.319 d_h)]}{X} + \frac{1}{X^2} \right\}} \quad (29)$$

It should be noted that the units of the hydraulic diameter (d_h) in the above equation are in mm. In Eq. (29), Nusselt numbers for thermally developed laminar flow with three-sided and four-sided heat transfer (Nu_3 and Nu_4), respectively, are defined as follows [82]:

$$Nu_3 = 8.235(1 - 1.833AR + 3.767AR^2 - 5.814AR^3 + 5.361AR^4 - 2.0AR^5) \quad (30)$$

$$Nu_4 = 8.235(1 - 2.042AR + 3.085AR^2 - 2.477AR^3 + 1.058AR^4 - 0.186AR^5) \quad (31)$$

The Fanning friction factor (f) based on liquid flow can be determined as follows:

$$f\mathrm{Re_l} = 24(1 - 1.3553AR + 1.9467AR^2 - 1.7012AR^3 + 0.9564AR^4 - 0.2537AR^5) \quad \mathrm{Re_l} < 2000 \quad (32)$$

$$f = \frac{0.079}{\mathrm{Re_l^{0.25}}} \quad 2000 \le \mathrm{Re_l} < 20,000 \quad (33)$$

$$f = \frac{0.046}{\mathrm{Re_l^{0.2}}} \quad \mathrm{Re_l} \ge 20,000 \quad (34)$$

$$\mathrm{Re_l} = \frac{G(1-x)d_h}{\mu_l} \quad (35)$$

In the Shah and London relation [82] for laminar flow forced convection in rectangular ducts, Eq. (32), AR = 0 is the case of parallel plates and $f_k\mathrm{Re}_k = 24$ in that case while AR = 1 is the case of square shape and $f_k\mathrm{Re}_k = 14.23$ in that case.

In order to further assess the accuracy of their new annular condensation heat transfer correlation, Eq. (29), Kim and Mudawar [81] amassed a total 923 data points for condensation in mini/microchannels from eight sources. The researchers plotted all 923 data points in the form of the Lockhart–Martinelli parameter based on turbulent liquid-turbulent vapor (X_{tt}) versus modified Weber number (We*). In the plot in Fig. 1, the liquid and vapor Reynolds numbers ($\mathrm{Re_l}$ and $\mathrm{Re_g}$) of the 923 data points were classified either laminar or turbulent with a transition Reynolds number value of 2000. The modified Weber number (We*) was defined by Soliman [62] as follows:

$$\mathrm{We}^* = 2.45\frac{\mathrm{Re_g^{0.64}}}{\mathrm{Su_g^{0.3}}(1 + 1.09X_{tt}^{0.039})^{0.4}} \quad \mathrm{Re_l} \le 1250 \quad (36)$$

$$\mathrm{We}^* = 8.5\frac{\mathrm{Re_g^{0.79}}X_{tt}^{1.57}}{\mathrm{Su_g^{0.3}}(1 + 1.09X_{tt}^{0.039})^{0.4}}\left[\left(\frac{\mu_g}{\mu_l}\right)^2\left(\frac{\rho_l}{\rho_g}\right)\right] \quad \mathrm{Re_l} > 1250 \quad (37)$$

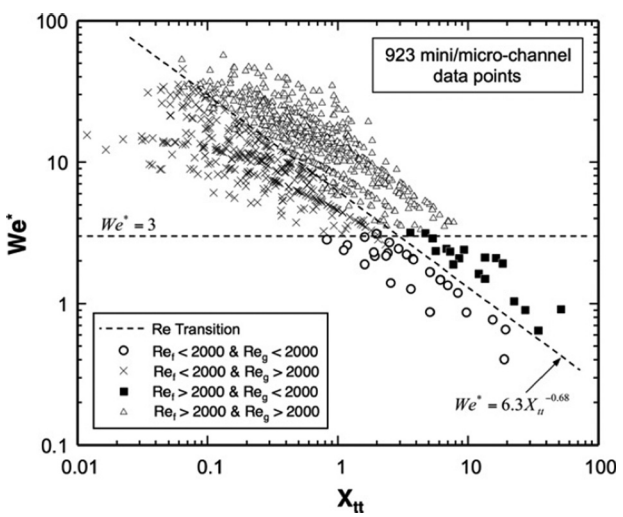

Fig. 1 Reynolds number transition lines based on 923 mini/microchannel data points from eight sources. Reprinted with permission from Kim, S.-M., and Mudawar, I., 2012, "Flow Condensation in Parallel Micro-Channels—Part 2: Heat Transfer Results and Correlation Technique," Int. J. Heat Mass Transfer, 55(4), pp. 984–994. Copyright 2012 Elsevier) [81].

In the equations of the modified Weber number (We*), the Reynolds number for vapor flow ($\mathrm{Re_g}$), the Suratman number for vapor flow ($\mathrm{Su_g}$), and the Lockhart–Martinelli parameter based on turbulent liquid-turbulent vapor (X_{tt}) were defined as

$$\mathrm{Re_g} = \frac{Gxd_h}{\mu_g} \quad (38)$$

$$\mathrm{Su_g} = \frac{\rho_g\sigma d_h}{\mu_g^2} \quad (39)$$

$$X_{tt} = \left(\frac{1-x}{x}\right)^{0.9}\left(\frac{\rho_g}{\rho_l}\right)^{0.5}\left(\frac{\mu_l}{\mu_g}\right)^{0.1} \quad (40)$$

It should be noted that although all the data were plotted versus the Lockhart–Martinelli parameter based on turbulent liquid-turbulent vapor (X_{tt}), they were classified clearly into the following four various zones by two fitted lines of We* = 3 and We* = 6.3 $X_{tt}^{-0.68}$. The first zone for laminar liquid-laminar vapor flow ($\mathrm{Re_l} < 2000$ and $\mathrm{Re_g} < 2000$) was described by the following relation:

$$\mathrm{We}^* < 3 \quad \text{and} \quad \mathrm{We}^* < 6.3X_{tt}^{-0.68} \quad (41)$$

The second zone for laminar liquid-turbulent vapor flow ($\mathrm{Re_l} < 2000$ and $\mathrm{Re_g} > 2000$) was described by the following relation:

$$3 < \mathrm{We}^* < 6.3X_{tt}^{-0.68} \quad (42)$$

The third zone for turbulent liquid-laminar vapor flow ($\mathrm{Re_l} > 2000$ and $\mathrm{Re_g} < 2000$) was described by the following relation:

$$6.3X_{tt}^{-0.68} < \mathrm{We}^* < 3 \quad (43)$$

The fourth zone for turbulent liquid-turbulent vapor flow ($\mathrm{Re_l} > 2000$ and $\mathrm{Re_g} > 2000$) was described by the following relation:

$$\mathrm{We}^* > 3 \quad \text{and} \quad \mathrm{We}^* > 6.3X_{tt}^{-0.68} \quad (44)$$

Based on the FC72 flow visualization data presented in the first part of their study [80], the following lines are fitted for boundaries between various flow regimes:

For smooth—annular to wavy—annular

$$\mathrm{We}^* = 90X_{tt}^{0.5} \quad (45)$$

For wavy-annular to transition

$$\mathrm{We}^* = 24X_{tt}^{0.41} \quad (46)$$

For transition to slug

$$\mathrm{We}^* = 7X_{tt}^{0.2} \quad (47)$$

Cavallini et al. [83] proposed that the flow was annular for the dimensionless superficial vapor velocity (J_g^*) > 2.5, and intermittent and slug for $J_g^* < 2.5$, based on previous flow regime maps. The dimensionless superficial vapor velocity (J_g^*) was defined as follows:

$$J_g^* = \frac{Gx}{\sqrt{\rho_g(\rho_l - \rho_g)gd_h}} \quad (48)$$

Kim and Mudawar [81] showed proposed flow regime map based on their FC72 flow visualization experiments in square

microchannels with $d_h = 1$ mm plotted alongside 639 mini/microchannel annular data points corresponding to $J_g^* > 2.5$ from eight aforementioned sources with excluding all data with $J_g^* < 2.5$ as shown in Fig. 2. Although a few data points did appear for $We^* < 7\,X_{tt}^{-0.2}$, the boundary line between the transition and slug regimes from their study was in general agreement with that from Cavallini et al. [83].

Kim and Mudawar [81] mentioned that their new correlation showed excellent predictive capability based on both the present FC72 data and a large database for mini/microchannel flows amassed from eight previous sources.

Kuczyński et al. [84] presented the results of an investigation of the effect of hydrodynamic instabilities on heat transfer intensity during the condensation of R134a and R404A refrigerants in horizontal pipe minichannels with internal diameters of $d = 0.64$, 0.90, 1.40, 1.44, 1.92, 2.30, and 3.30 mm. The researchers induced disturbances of the condensation process with a periodic stop and a repetition of the refrigerant flow. They identified an unfavorable effect on the intensity of the heat transfer during the condensation process in pipe minichannels in the range of frequencies, $f = 0.25$–5 Hz, of the periodically generated disturbances, The reduction in the intensity of the heat transfer during the condensation process that was induced with hydrodynamic instabilities, was presented in the form of the dependence of the heat transfer coefficient (h) on the vapor quality (x) and the frequencies (f) of the disturbances. Also, they identified the effect of the refrigerant, the diameter of the minichannels and the frequency (f) on the damping phenomenon of the periodical disturbances in the pipe minichannels.

Fronk and Garimella [85] investigated experimentally heat transfer and pressure drop during condensation of ammonia in a single circular tube of $d = 1.435$ mm. The researchers chose NH_3 as a working fluid because of its use in thermal systems was attractive due to its high latent heat, favorable transport properties, zero ozone depletion, and zero global warming potential (GWP) as well as there were few data on condensation of ammonia at the microscale while there was a growing body of research on condensation of conventional refrigerants (i.e., R134a, R404A, etc.) in microchannels. Ammonia has significantly different fluid properties than synthetic hydrofluorocarbon and hydrochlorofluorocarbon refrigerants. For example, at $T_s = 60\,^{\circ}C$, ammonia has a surface tension 3.2 times and an enthalpy of vaporization 7.2 times greater than those of R134a. Therefore, models validated with data for synthetic refrigerants might not predict condensation of ammonia with sufficient accuracy. Their test section consisted of a stainless steel tube-in-tube heat exchanger with ammonia flowing through a microchannel inner tube and cooling water flowing through the annulus in counterflow. They maintained a high flow rate of water to provide an approximately isothermal heat sink and to ensure the condensation thermal resistance dominated the heat transfer process. They determined condensation heat transfer coefficient and two-phase frictional pressure gradient at mass fluxes (G) of 75 and 150 kg/(m$^2 \cdot$ s), multiple saturation temperatures (corresponding to $P_r = 0.10$–0.23), and in small quality increments ($\Delta x \sim$ 15–25%) from 0 to 1. They discussed trends in heat transfer coefficients and pressure drops and used the results to assess the applicability of models developed for both macro and microscale geometries for predicting the condensation of ammonia. The dependence of pressure drop and heat transfer on mass quality and mass flux was as expected. However, they found that existing models were not able to accurately predict the results. The coupled influences of ammonia properties and microscale geometry were outside the applicable range of most condensation heat transfer and pressure drop models. Additional reliable data heat transfer and pressure drop for smaller tube diameters and with working fluids like ammonia were necessary. These results would enable the development of models, which allow better prediction of condensation over a wider range of working fluids, operating conditions, and hydraulic diameters.

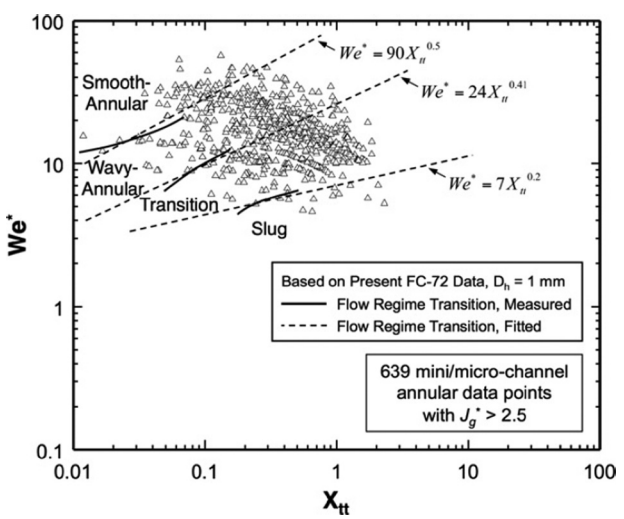

Fig. 2 Proposed flow regime map based on present FC72 flow visualization experiments in square microchannels with the hydraulic diameter of 1 mm plotted alongside 639 minichannel/microchannel data points corresponding to $J_g^* > 2.5$ from eight sources. Reprinted with permission from Kim, S.-M., and Mudawar, I., 2012, "Flow Condensation in Parallel Micro-Channels—Part 2: Heat Transfer Results and Correlation Technique," Int. J. Heat Mass Transfer, 55(4), pp. 984–994. Copyright 2012 Elsevier) [81].

Da Riva and Del Col [86] presented a three-dimensional volume of fluid (VOF) simulation of condensation of R134a in a horizontal circular 1 mm minichannel at mass flux (G) = 100 kg/(m$^2 \cdot$ s) with taking into account the gravity effect. The researchers run simulations both with and without taking into account surface tension. They fixed a uniform interface temperature and a uniform wall temperature as boundary conditions. They assumed that the flow was laminar inside the liquid phase and turbulent inside the vapor phase. They handled turbulence inside the vapor phase by a modified low Reynolds form of the k–ω model. The fluid was condensed till arriving at mass quality (x) = 0.45. They expected that the flow to be annular without the presence of waves, therefore they treated the problem as steady state. They reported and validated their computational results displaying the evolution of vapor–liquid interface and heat transfer coefficient against experimental data. They found that the condensation process to be gravity dominated, while the global influence of surface tension to be negligible. The liquid film was thin and evenly distributed all around the tube circumference at inlet. Moving downstream the channel, the film thickness remained almost constant in the upper half of the minichannel, while the film at the bottom of the pipe became thicker because the liquid condensed at the top was drained by gravity to the bottom.

Nebuloni and Thome [87] presented numerical simulations of annular laminar film condensation heat transfer in microchannels of various internal shapes. Their model, which was based on a finite volume formulation of the Navier–Stokes and energy equations for the liquid phase only, importantly accounted for the influences of axial and peripheral wall conduction and nonuniform heat flux not included in other models so far in the literature. The researchers included the contributions of the surface tension, axial shear stresses, and gravitational forces. They validated their model versus different benchmark cases and versus experimental data available in literature. The prediction of the microchannel heat transfer data using their model had an average error of 20% or better. It was well known that the condensate film thinning induced by surface tension due to gravity forces and shape of the surface, also known as the "Gregorig" influence, had a strong consequence on the local heat transfer coefficient in condensation. Therefore, their model accounted for these influences on the heat transfer and pressure drop for a wide variety of geometrical shapes, sizes, wall materials, and working fluid properties. In their paper, they

studied the conjugate heat transfer problem arising from the coupling between the thin film fluid dynamics, the heat transfer in the condensing fluid, and the heat conduction in the channel wall. In particular, they presented three external channel wall boundary conditions: a uniform wall temperature, a nonuniform wall heat flux, and single-phase convective cooling. As the scale of the problem was reduced, i.e., when moving from minichannel to microchannels, their results showed that the axial conduction influences could become very important in the prediction of the wall temperature profile and the magnitude of the heat transfer coefficient and its distribution along the channel.

Zhang et al. [88] investigated experimentally condensation heat transfer and pressure drop of R22, R410A, and R407C in two single round stainless steel tubes with $d = 1.088$ mm and 1.289 mm. The researchers measured condensation heat transfer coefficients and two-phase pressure drop at the saturation temperatures of 30 °C and 40 °C. The mass flux (G) varied from 300 to 600 kg/($m^2 \cdot s$) and the vapor quality (x) 0.1–0.9. They investigated the influences of mass flux and vapor quality and their results indicated that condensation heat transfer coefficients increased with mass flux and vapor quality, increasing faster in the high vapor quality region. They compared their experimental data with the correlations based on experimental data from large diameter tubes ($d_h > 3$ mm), like the Shah [15] and Akers et al. [12] correlations. Almost all the correlations overestimated their experimental data, but Wang et al. correlation [20] and Yan and Lin correlation [16] that were developed based on the experimental data from mini-tubes predicted their experimental data reasonably well. Condensation heat transfer coefficients and two-phase pressure drop of R22 and R407C were equivalent but both higher than those of R410A. As a substitute for R22, R410A had more advantages than R407C in view of the characteristics of condensation heat transfer and pressure drop.

Del Col et al. [89] presented an experimental investigation on condensation of R134a inside a single square cross section minichannel when varying the channel orientation. The researchers measured local heat transfer coefficients in horizontal configuration, vertical downflow, and 45 deg downwards. They carried out this study because the number of local heat transfer coefficient values measured during condensation inside noncircular minichannels in the literature was rather limited and the channel orientation effect during condensation was not much investigated. They employed an accurate experimental technique to assess the channel orientation effect on the heat transfer coefficients during condensation of R134a at 40 °C saturation temperature inside a square cross section minichannel, with a hydraulic diameter (d_h) of 1.23 mm. They reported local heat transfer coefficients at mass fluxes (G) between 100 kg/($m^2 \cdot s$) and 790 kg/($m^2 \cdot s$) for three various configurations: horizontal, vertical downflow, and 45 deg inclination downflow. By taking into account the experimental uncertainty, they noticed no differences for the three configurations at high mass fluxes down to 200 kg/($m^2 \cdot s$). On the other hand, the heat transfer coefficients at 100 kg/($m^2 \cdot s$) in vertical and 45 deg inclination downflow were lower as compared to the ones measured in the horizontal channel.

In the literature, the number of local heat transfer coefficient values measured during condensation inside noncircular minichannels was rather limited and the channel orientation effect during condensation was not much investigated. Some studies have been performed in inclined smooth tubes of larger diameters, where it was shown that the heat transfer coefficient was strongly influenced by the liquid and vapor distributions. But minichannels might display a various behavior because of the relative importance of shear stress, gravity and surface tension. The action of these forces might be dependent on operating conditions and orientation. In this study, Del Col et al. [90] presented an experimental investigation of condensation of R134a inside a single square cross section minichannel when varying the channel orientation. The researchers measured local heat transfer coefficients in horizontal, vertical downflow, and vertical upflow configurations. They obtained the channel from a copper rod and had a square cross section with 1.18 mm side length. Every corner had a curvature radius equal to 0.15 mm that led to a hydraulic diameter (d_h) equal to 1.23 mm. They performed tests with R134a as the working fluid at saturation temperature (T_s) of 40 °C, at mass flux (G) ranging between 100 and 790 kg/($m^2 \cdot s$). From the experimental results, they investigated the channel inclination effect when varying mass flux and vapor quality. According to the experimental uncertainty, they noticed no differences for the three configurations at mass fluxes from 790 kg/($m^2 \cdot s$) down to 200 kg/($m^2 \cdot s$), where the condensation heat transfer was controlled by shear stress and surface tension. On the other hand, the heat transfer coefficients at 100 and 135 kg/($m^2 \cdot s$) in vertical downflow were lower as compared to the ones measured in the horizontal configuration and vertical upflow.

Odaymet et al. [91] investigated condensation of steam in a single silicon microchannel using a simultaneous condensate flow visualization and heat transfer measurement along the flow direction. The researchers used a silicon microchannel of a rectangular cross section covered with a transparent Pyrex glass. They identified various condensate flow patterns like mist flow, churn flow, upstream elongated bubble flow followed by a bubble sequence, and slug flow. Both surface temperature measurements and video images obtained for various flows showed that the condensate flows were periodic or stable during time. The local surface temperature, local heat flux, and local heat transfer coefficient related to various condensate flow patterns were of particular interest. They deduced the local heat transfer coefficient from the local heat flux and measured the local surface temperature through micro-instrumentation in a microchannel. They found that local thermal performance of condensation flow in a microchannel was better for mist flow and upstream elongated bubble flow relative to slug and bubbly flows.

Hu et al. [92] presented an analysis of condensation heat transfer model in small channels. The researchers addressed nine condensation heat transfer prediction models of small channels, and setup a database by collecting 1183 condensation heat transfer data points of small channels that involved six types of refrigerants (R134a, R32, R22, R123, R410A, and R1234yf) from 11 independent research groups. On basis of the comparison between the prediction results and the database, they found that most of prediction models could not capture the points of all fluids under different operating conditions in small channels. Therefore, proper model should be chosen according to refrigerants and operating conditions. For example, the Koyama et al. [23] model could almost fit for all data under most of the operating conditions within an acceptable deviation.

Zhang et al. [93] presented the flow condensation heat transfer characteristics of CO_2 in a minichannel condenser. The condenser consisted of seven tubes in parallel whose inner diameter was 0.9 mm that were thermally connected to two aluminum baseplates by using thermal glue. At saturation temperatures ranging from −5 °C to 15 °C, with mass fluxes of 180, 360, and 540 kg/($m^2 \cdot s$), respectively, and average vapor qualities from 0.2 to 0.8, they obtained the CO_2 condensation heat transfer coefficients, ranging from 1700 to 4500 W/(m^2·K). They compared the measured heat transfer coefficients with those predicted by the established correlations, and found that the Thome et al. model [51] was applicable to the condenser under investigation, with deviation less than 30%.

Kim and Mudawar [94] proposed a new universal approach to predict the condensation heat transfer coefficient for mini/microchannel flows, which was capable of tackling many fluids with drastically different thermophysical properties and very broad ranges of all geometrical and flow parameters of practical interest. First, the researchers amassed a consolidated database consisting of 4045 data points from 28 sources. This database consisted of single-channel and multichannel data, 17 various working fluids (R12, R123, R1234yf, R1234ze(E), R134a, R22, R236fa, R245fa, R32, R404A, R410A, R600a, FC72, methane, and CO_2), hydraulic

diameters (d_h) from 0.424 to 6.22 mm, mass fluxes (G) from 53 to 1403 kg/(m$^2\cdot$s), liquid-only Reynolds numbers (Re_{lo}) from 276 to 89,798, mass qualities (x) from 0 to 1, and reduced pressures (P_r) from 0.04 to 0.91. An exhaustive assessment of prior correlations showed only two correlations, which were actually intended for macrochannels, provided relatively fair predictions, while mini/microchannel correlations generally showed poor predictions. Therefore, they proposed two new correlations, one for predominantly annular flows, and the second for slug and bubbly flows. These two new correlations were

For annular flow (smooth-annular, wavy-annular, transition) where $We^* < 7\,X_{tt}^{-0.2}$

$$\frac{h_{ann}d_h}{k_l} = 0.048Re_l^{0.69}Pr_l^{0.34}\frac{\phi_g}{X_{tt}} \tag{49}$$

For slug and bubbly flows where $We^* < 7\,X_{tt}^{-0.2}$

$$\frac{h_{non-ann}d_h}{k_l} = \left[\left(0.048Re_l^{0.69}Pr_l^{0.34}\frac{\phi_g}{X_{tt}}\right)^2 + \left(3.2\times10^{-7}Re_l^{-0.38}Su_{go}^{1.39}\right)^2\right]^{0.5} \tag{50}$$

It should be noted that new nonannular correlation, Eq. (50), for the 713 slug and bubbly flow data points was superposition of the Churchill and Usagi [95] type of the new annular flow heat transfer correlation presented earlier for the 3332 annular data points, Eq. (49), and a dimensionless function of the superficial liquid Reynolds number (Re_l) and vapor-only Suratman number (Su_{go}) using the fitting or "blending" parameter of 2. Recently, Awad [96] summarized briefly the use of asymptotic method in many applications of two-phase flow. The equations for the different parameters in Eqs. (49) and (50) are given below:

$$X_{tt} = \left(\frac{1-x}{x}\right)^{0.9}\left(\frac{\rho_g}{\rho_l}\right)^{0.5}\left(\frac{\mu_l}{\mu_g}\right)^{0.1} \tag{51}$$

$$\phi_g^2 = 1 + CX + X^2 \tag{52}$$

$$X^2 = \frac{(dP/dz)_l}{(dP/dz)_g} \tag{53}$$

$$\left(\frac{dP}{dz}\right)_l = \frac{2f_lG^2(1-x)^2}{\rho_l d_h} \tag{54}$$

$$\left(\frac{dP}{dz}\right)_g = \frac{2f_gG^2x^2}{\rho_g d_h} \tag{55}$$

$$f_k = \frac{16}{Re_k} \quad Re_k < 2000 \tag{56}$$

$$f_k = \frac{0.079}{Re_k^{0.25}} \quad 2000 \le Re_k < 20,000 \tag{57}$$

$$f_k = \frac{0.046}{Re_k^{0.2}} \quad Re_k \ge 20,000 \tag{58}$$

For laminar flow forced convection in rectangular ducts, the Shah and London relation [82] can be used. This relation can be written as a function of the AR as follows:

$$f_kRe_k = 24(1 - 1.3553AR + 1.9467AR^2 - 1.7012AR^3 + 0.9564AR^4 - 0.2537AR^5) \tag{59}$$

where subscript k denotes l or g for liquid and vapor phases, respectively.

In Eq. (59), AR = 0 is the case of parallel plates and $f_kRe_k = 24$ in that case while AR = 1 is the case of square shape and $f_kRe_k = 14.23$ in that case

$$Re_l = \frac{G(1-x)d_h}{\mu_l} \tag{60}$$

$$Re_g = \frac{Gxd_h}{\mu_g} \tag{61}$$

The different correlations for C for different laminar and turbulent liquid and vapor flow states were

For turbulent liquid-turbulent vapor flow ($Re_l > 2000$ and $Re_g > 2000$)

$$C = 0.39Re_{lo}^{0.03}Su_{go}^{0.10}\left(\frac{\rho_l}{\rho_g}\right)^{0.35} \tag{62}$$

For turbulent liquid-turbulent vapor flow ($Re_l > 2000$ and $Re_g > 2000$)

$$C = 8.7\times10^{-4}Re_{lo}^{0.17}Su_{go}^{0.50}\left(\frac{\rho_l}{\rho_g}\right)^{0.14} \tag{63}$$

For laminar liquid-turbulent vapor flow ($Re_l < 2000$ and $Re_g > 2000$)

$$C = 0.0015Re_{lo}^{0.59}Su_{go}^{0.19}\left(\frac{\rho_l}{\rho_g}\right)^{0.36} \tag{64}$$

For laminar liquid-laminar vapor flow ($Re_l < 2000$ and $Re_g < 2000$)

$$C = 3.5\times10^{-5}Re_{lo}^{0.44}Su_{go}^{0.50}\left(\frac{\rho_l}{\rho_g}\right)^{0.48} \tag{65}$$

In the equations of the parameter (C), the Reynolds number for all flow as liquid (Re_{lo}), and the Suratman number for all flow as vapor (Su_{go}) were defined as

$$Re_{lo} = \frac{Gd_h}{\mu_l} \tag{66}$$

$$Su_{go} = \frac{\rho_g\sigma d_h}{\mu_g^2} \tag{67}$$

Kim and Mudawar [94] mentioned that their new annular correlation, Eq. (49), predicted the 3332 annular data points with a MAE of 15.9%, with 87.4% and 97.9% of the data falling within ±30% and ±50% error bands, respectively, while their new nonannular correlation, Eq. (50), predicted the 713 slug and bubbly flow data points with a MAE of 16.7%, with 83.9% and 97.5% of the data falling within ±30% and ±50% error bands, respectively. These low values of MAE could be attributed to the large database (4045 data points) upon which it was based. They showed that this accuracy was fairly even for various working fluids, and over broad ranges of hydraulic diameter, mass flux, mass quality and pressure, and for both single and multiple mini/microchannels.

Goss and Passos [97] investigated experimentally the local heat transfer coefficient during the convective condensation of R134a inside eight round (diameter $d = 0.77$ mm) horizontal and parallel microchannels. The test conditions included the pressure (P), the mass quality (x), the heat flux (q), and the mass flux (G) ranging from 7.3 to 9.7 bar, 0.55 to 1, 17 to 53 kW/m^2, and 230 to 445 kg/(m$^2\cdot$s), respectively. The researchers evaluated the effect of

temperature, heat flux, mass flux and mass quality on the heat transfer coefficient (h). Their results showed that mass flux and mass quality had an important effect on the heat transfer coefficient. The consideration that all of the resistance to heat transfer was due to the conduction through the liquid film was a good approximation, mainly for $x < 0.95$. Also, they compared their experimental results with correlations and semi-empirical models described in the literature.

The relative magnitudes of the forces governing the transfer of heat, mass, and momentum during microscale condensation were fundamentally different from those in macroscale geometries, primarily due to the increasing importance of surface tension. As a result, Garimella and Fronk [98] conducted a systematic series of experiments on condensation flow regimes, pressure drop, and heat transfer using innovative visualization and measurement techniques for condensation of synthetic and natural refrigerants and their azeotropic and zeotropic mixtures through microchannels with a wide range of diameters ($0.1 < d_h < 5$ mm), shapes, and operating conditions. These experiments resulted in flow-regime-based heat transfer and pressure drop models with very good predictive capabilities for such microchannel geometries.

Wang and Rose [99] investigated heat transfer and pressure drop during laminar annular flow condensation in microchannels. The special case of annular laminar condensate flow permitted wholly theoretical solution without recourse to empirical input. For laminar annular flow condensation in microchannels and for specified fluid, channel geometry, flow parameters and tube wall temperatures, local heat transfer coefficient, and local pressure gradient could be calculated as well as local quality and void fraction. The researchers outlined the theory in this paper, and discussed recent developments. They summarized and compared results for heat transfer and pressure drop for laminar annular flow condensation in microchannels with experimental data. They found that correlations of experimental data for both heat transfer and pressure drop could only be expected to have validity for fluids and conditions close to those used when obtaining the data on which the correlations were based. For the heat transfer coefficient, they found that the results of the annular flow theory were in surprisingly good agreement with the correlations when applied to R134a. For ammonia, the theoretical results lay between the widely spread values obtained from the correlations.

Liu et al. [100] investigated experimentally heat transfer characteristics of R152a during condensation in a 1.152 mm circular stainless steel microchannel. The researchers conducted tests with saturation temperatures (T_s) of 40 to 50 °C, mass fluxes (G) of 200 to 1200 kg/(m^2 · s) and vapor qualities (x) of 0.1 to 0.9. They investigated effects of mass flux, vapor quality, saturation temperature, heat flux, and inclination angle on heat transfer coefficients. They found that heat transfer coefficients increased with mass flux and vapor quality while decreased with saturation temperature and heat flux. Inclination angle enhanced condensation heat transfer at low mass fluxes. They compared their data with existing correlations and predictive deviations were large. Based on their data, they modified one heat transfer correlation and predictive deviations were within ±30%.

Liu et al. [101] presented experimental data for heat transfer and pressure drop during condensation of R152a in circular and square microchannels with hydraulic diameters (d_h) of 1.152 mm and 0.952 mm, respectively. Saturation temperatures (T_s) were 40 °C and 50 °C with mass fluxes (G) varying from 200 to 800 kg/(m^2 · s) and vapor mass qualities (x) from 0.1 to 0.9. The researchers investigated effects of mass flux, vapor mass quality and channel geometry on heat transfer and pressure drop. They found that heat transfer coefficients and pressure gradients during condensation increased with increasing mass flux and vapor mass quality while decreased with increasing saturation temperature both in circular and square microchannels. The heat transfer coefficients of the square microchannel were higher than those of the circular microchannel at $G = 200$ kg/(m^2 · s) and 400 kg/(m^2 · s) due to the surface tension effect. The heat transfer enhancement decreased with mass flux as the shear stress played a much more important role at higher mass fluxes. However, channel geometry had little influence on two-phase pressure gradients. They compared their experimental data with earlier empirical correlations and a theoretical solution. They found that the heat transfer results for the circular microchannel agreed within experimental error with Wang et al. [20] and Koyama et al. [23] correlations and the theoretical solution of Rose and Wang [9], while for the square microchannel their results agreed within experimental error with Koyama et al. [23], Cavallini et al. [67], and Bandhauer et al. [36] correlations and the theoretical solution of Rose and Wang [9].

Yun et al. [102] investigated influences of two-phase flow patterns and oil concentration (PAG type) on the heat transfer coefficient and pressure drop of CO_2 under condensation in microchannel. The hydraulic diameter (d_h) of the microchannel having 19 rectangular channels was 0.68 mm, and the oil concentrations ranged from 0.7 to 1.2 wt.%. From the data collected, the researchers developed a prediction model of CO_2 condensation heat transfer coefficient in microchannels by considering the effects of liquid film thickness, and of the interface shape between liquid and gas phases on heat transfer coefficient. They utilized the narrow single rectangular channel whose dimension is 16×2 mm to observe the flow patterns of CO_2 under condensation. The transition vapor quality from intermittent flow to annular flow became advanced with increase of mass flux and with decrease of condensation temperature. Also, they found that the heat transfer coefficient decreased with oil concentration. It decreased by 50% as compared to that of the pure CO_2 when mass flux (G) was 600 kg/(m^2 · s), and oil concentration was changed from 0.7 to 1.2 wt.%. In contrast, the pressure drop slightly increased with oil concentration as compared to that of pure CO_2. This phenomenon was also observed in other existing studies. For the heat transfer in microchannels, they obtained the data utilized to develop the heat transfer coefficient model from present test and previous other studies. Total number of data was 346. The hydraulic diameters of microchannels ranged from 0.68 to 1.5 mm. Their prediction model estimated the experimental data within 18.9% of mean deviation.

Heo et al. [103] investigated the condensation heat transfer coefficient and pressure drop of CO_2 in a multiport microchannel with a hydraulic diameter (d_h) of 1.5 mm with variation of the mass flux (G) from 400 to 1000 kg/(m^2 · s) and of the condensation temperature (T) from −5 to 5 °C. The researchers found that the heat transfer coefficient and pressure drop increased with the decrease of condensation temperature and the increase of mass flux. However, the increase rate of the heat transfer coefficient was retarded by these changes. The gradient of the pressure drop with respect to vapor quality (x) was significant with the increase of mass flux (G). The existing models for heat transfer coefficient overpredicted their experimental data, and the deviation increased at high vapor quality and at high heat transfer coefficient. They found that Thome et al. model [51] gave the smallest mean deviation of ±51.8%.

El Achkar et al. [104] investigated flow patterns and heat transfer during condensation of n-pentane in an air-cooled square cross section microcondenser. The test section consisted of a borosilicate square microchannel, of inner and outer edges 553 μm and 675 μm, respectively, and of a length 208 mm. The transparency of the microchannel walls allowed the visualization of the phases distribution and the various condensation flow regimes. The mass flux (G) range was between 3 and 15 kg/(m^2 · s). The researchers identified three main flow regimes: annular regime, intermittent regime, and spherical bubbles regime. They developed a specific experimental procedure, based on bubbles tracking, to determine accurately the hydraulic and thermal parameters profiles in the isolated bubbles zone, like the time-averaged void fraction profile and the time-averaged vapor quality profile, according to the axial position in the microchannel. They determined the time-averaged liquid temperature profile in the isolated bubbles zone using the energy balance. A significant temperature difference between the

liquid and vapor phases was highlighted. Therefore, they quantified and compared the latent and total heat fluxes released in this zone to every other. Besides, they determined and compared the relationship between the void fraction and the vapor quality in the spherical bubbles zone to existing void fraction models. Finally, they determined the bubbles detachment frequency. A relationship between this frequency and the mass flux was proposed.

Ganapathy et al. [105] presented a numerical model for the simulation of condensation heat transfer and fluid flow characteristics in a single microchannel. The researchers based their model on the VOF approach that governed the hydrodynamics of the two-phase flow. They governed the condensation characteristics using the physics of the phenomena and excluded any empirical expressions in the formulation. They modified the conventional governing equations for conservation of volume fraction and energy to include source terms, which accounted for the mass transfer at the liquid–vapor interface and the associated release of latent heat, respectively. They modeled a microchannel having characteristic dimension of 100 μm using a two-dimensional computational domain. The working fluid was R134a and the vapor mass flux (G_g) at the channel inlet ranged from 245 to 615 kg/(m^2 · s). The channel wall was maintained at a constant heat flux (q) ranging from 200 to 800 kW/m^2. They assessed the predictive accuracy of their numerical model by comparing the two-phase frictional pressure drop and Nusselt number with available empirical correlations in the literature. They obtained a reasonably good agreement for both parameters with a MAE of 16.6% for Nusselt number against the Dobson and Chato correlation [106]. Furthermore, a qualitative comparison of different flow patterns against experimental visualization data also indicated a favorable agreement.

Heo et al. [107] presented comparison of condensation heat transfer and pressure drop of CO_2 in three various microchannels. The channels were rectangular, and the numbers of ports were 7, 19, and 23. The hydraulic diameters (d_h) were 1.5, 0.78, and 0.68 mm for the 7, 23, and 19 ports, respectively. The test temperature ranged from −5 to 5 °C, and the range of the mass flux (G) was from 400 to 800 kg/(m^2 · s). The researchers found that the condensation heat transfer coefficient increased with the decrease in hydraulic diameter (d_h) that was dominant at condensation temperatures of 0 and −5 °C. They observed increasing and decreasing the heat transfer coefficient at critical vapor quality for the microchannel of 23 ports. Also, they found the highest pressure drop in the microchannel of 23 ports too. The Thome et al. model [51] showed the smallest mean deviation of 47.7% for the heat transfer coefficient.

Rose and Wang [108] compared detailed experimental investigations of condensation in microchannels where local heat flux and surface temperature were measured along the channel with theoretical results for the special case of annular, laminar flow. Their theoretical model included surface tension driven transverse flow towards the corners of the channel as well as shear stress driven streamwise flow in an otherwise Nusselt treatment. This theory had no empirical input. When distributions along the channel of the local vapor and wall temperatures were given, local heat flux and heat transfer coefficient, as well as local vapor quality, might be calculated. Such detailed experimental data had only recently become available. Strict implementation of the theory required that the condensation onset occurred within the channel, i.e., the vapor is saturated or superheated at the inlet. Their comparisons showed remarkably good agreement with the experimental data for two fluids and covering a wide range of experimental conditions.

Dang and Doan [109] investigated experimentally condensation heat transfer of two microchannel heat exchangers with rectangular channels having hydraulic diameters (d_h) of 375 μm and 265 μm. The heat transfer rate of a microchannel heat exchanger was achieved 272.9 W for the vapor having the inlet temperature of 101 °C and the mass flow rate of 0.123 g/s and for the cooling water having the inlet temperature of 32 °C and mass flow rate of 3.1133 g/s. Also, the researchers observed that the heat transfer rate obtained from the counter-flow arrangement was always higher than that obtained from the parallel one: the value obtained from the counter-flow arrangement is 1.04 to 1.05 times of that obtained from the parallel flow. They found that the results for two phases were in good agreement with the results for single phase. However, they showed that the flow arrangement effect in two phases was not stronger than single phase. In addition, the condensation heat transfer coefficient in the microchannel heat exchangers decreased as increasing the inlet cooling water temperature.

Bortolin et al. [110] proposed a number of steady-state numerical simulations of condensation of R134a at mass fluxes of 400 kg/(m^2 · s) and 800 kg/(m^2 · s) inside a 1-mm square cross section minichannel and compared against simulations in a circular cross section channel with the same hydraulic diameter. The researchers used the VOF method to track the vapor–liquid interface, and took into account the influences of interfacial shear stress, surface tension, and gravity. A uniform wall temperature was fixed as a boundary condition. They treated the liquid film and the vapor core at both mass fluxes as turbulent and used a low-Re form of the shear stress transport k-ω model by Menter [111] for the modeling of turbulence through both the liquid and vapor phases. They validated numerical simulations against experimental data. The effect of the surface tension on the shape of the vapor–liquid interface might provide some heat transfer enhancement in a square cross section minichannel, but this was dependent on the mass flux and it might be not significant at high mass flux, as confirmed by experimental data and by their numerical work. The gravity force was shown to be responsible for the liquid film thickness increase at the bottom of the channel in the circular cross section, but the gravity force had a minor influence in the square minichannel. At these mass fluxes, the heat transfer mechanism was dominated by shear stress and surface tension.

Derby et al. [112] examined the flow condensation enhancement of steam on hydrophobic and hydrophilic surfaces. The researchers tested six 1.06 mm minigaps at pressures of 350–400 kPa, average qualities of 0.2–0.95 and mass fluxes of 50–200 kg/(m^2 · s). The surfaces included hydrophilic copper, hydrophobic Teflon AF™, and four surfaces with combined Teflon and hydrophilic patterns. They guided pattern selection by an analytical model. They found that condensing heat transfer coefficients on hydrophobic and hydrophobic/hydrophilic patterned surfaces reached a value of up to 425,000 W/m^2 · K, surpassing the hydrophilic surface by an order of magnitude. Also, they found that enhancement factors of 3.2–13.4 times that of the hydrophilic channel in the hydrophobic channel. The data strongly suggested that dropwise condensation was promoted and sustained throughout the flow condensation process on hydrophobic and patterned surfaces combined with a lack of dependence on mass flux or quality. For the hydrophilic copper minigap, heat transfer coefficients were a strong function of quality, as well as a function of mass flux at higher qualities that demonstrated the development and growth of a liquid film as quality decreased, and were well predicted by Kim and Mudawar [94] correlation, with a MAE of 8.9%.

El Mghari et al. [113] conducted numerical investigation of steam condensation in a noncircular microchannel. The researchers solved the conservation equation of mass, momentum and energy in both phases for different microchannel hydraulic diameters. They evaluated various correlations established for condensation flow heat transfer. They found that the correlation of Dobson et al. [114] and Koyama et al. [23] were the closest to the calculated steam condensation average heat transfer. They gave results for various microchannels shapes, AR, and for different inlet vapor mass fluxes and contact angle. Reducing the microchannel hydraulic diameter from 250 to 80 μm decreased the condensate film thickness and increased the average heat transfer coefficient up to 39% for the same mass flux. The enhancement factor of the heat transfer coefficient arrived to 100% by increasing the contact angle from 6 deg to 15 deg. The microchannel shape effect on the

Table 1 Summary of previous studies on condensation heat transfer in microchannels and minichannels

Author	d	Fluids	Orientation/conditions	Range/applicability	Techniques, basis, observations
Yang and Webb [10]	2.637 mm (plain tubes) 1.564 mm (tubes with microfins)	R12	Horizontal	$x = 0.12$–0.97 $G = 400$–$1400\,\mathrm{kg/(m^2 \cdot s)}$ $q = 4$–$12\,\mathrm{kW/m^2}$	At low mass flux, the Akers et al. correlation [12] agreed well with the plain tube data, and overpredicted the data 10–20% at high mass flux.
Webb and Zhang [13]	0.1–2.0 mm	Different refrigerants such as R134a	Horizontal		Their recently developed "equivalent Reynolds number ($\mathrm{Re_{eq}}$) model" [14] would predict the condensation coefficient of different refrigerants in tube diameters as small as 2.13 mm. The 1979 Shah equation [15] began to fail for R134a at $P/P_{cr} \geq 0.44$.
Yan and Lin [16]	2.0 mm	R134a	Horizontal	$L = 100$ mm $T_{sat} = 25$–$50\,^{\circ}\mathrm{C}$ $G = 100$–$200\,\mathrm{kg/(m^2 \cdot s)}$ $q = 10$–$20\,\mathrm{kW/m^2}$	$\frac{h_{tp}d}{k_l}\mathrm{Pr_l^{-0.33}Bo^{0.3}Re} = 6.48\mathrm{Re_{eq}^{1.04}}$.
Webb and Ermis [17]	0.44–1.56 mm	R134a	Horizontal	$G = 300$–$1000\,\mathrm{kg/(m^2 \cdot s)}$ $x = 15$–90%	The condensation coefficient increased with decreasing hydraulic diameter for the four tubes.
Zhao and Liao [19]	1.16, 0.87, and 0.58 mm	Steam	Vertical	$T_{sat} = 100\,^{\circ}\mathrm{C}$	The axial variation of the cross-sectional average heat transfer coefficient inside an equilateral triangular channel is substantially higher than that inside a round tube having the same hydraulic diameter, in particular in the entry region.
Wang et al. [20]	1.46 mm	R134a	Horizontal	$G = 75$–$750\,\mathrm{kg/(m^2 \cdot s)}$ $x = 3$–94%	They developed two correlations, each representing the physics of the specific phase distributions, to predict the heat transfer data (one for annular flow and the other for stratified flow). They proposed successfully a weighting correlation to account for all data regardless of the mix of flow regimes experienced.
Riehl et al. [21]	1.5 mm	Methanol (CH_3OH)	Horizontal		Microchannel condensers with a porous boundary can be used for heat dissipation with reduced heat transfer area and very high heat dissipation capabilities.
Riehl and Ochterbeck [22]	1.5, 1, 0.75, and 0.5 mm	Methanol (CH_3OH)	Horizontal	$T_{sat} = 45, 55\,^{\circ}\mathrm{C}$	Obtaining an empirical correlation to calculate the Nusselt number as a function of Weber, Jacob, Reynolds, and Prandtl numbers, respectively.
Koyama et al. [23]	1.114 mm (8 channels) 0.807 mm (19 channels)	R134a	Horizontal	$G = 100$–$700\,\mathrm{kg/(m^2 \cdot s)}$ $x = 0$–100%	$\frac{h_{tp}d}{k_l} = 0.0152(1 + 0.6\mathrm{Pr_l^{0.8}})* \frac{\phi_g}{X_{tt}}\mathrm{Re_l^{0.77}}$.
Garimella [26]	0.4–4.91 mm	R134a	Horizontal	$G = 150$–$750\,\mathrm{kg/(m^2 \cdot s)}$ $x = 0$–100%	Garimella [26] developed models for these measured heat transfer coefficients using the documented flow mechanisms and the corresponding pressure drop models as the basis.
Shin and Kim [27]	0.691 mm	R134a	Horizontal	$G = 100$–$600\,\mathrm{kg/(m^2 \cdot s)}$ $q = 5$–$20\,\mathrm{kW/m^2}$ $T_{sat} = 40\,^{\circ}\mathrm{C}$ $x = 15$–85%	Comparisons of experimental data with existing heat transfer correlations reveal that both the Shah [14] and the Petukhov [11] correlations failed to predict the present data.
Haui and Koyama [28]	1.31 mm	CO_2	Horizontal	$P = 6.48$–7.3 MPa $T_{inlet} = 21.63$–$31.33\,^{\circ}\mathrm{C}$ $q = 1.10$–$8.12\,\mathrm{kW/m^2}$ $G = 123.2$–$315.2\,\mathrm{kg/(m^2 \cdot s)}$ $x = 0$–100%	The existing model failed to predict the experimental data.
Shin and Kim [30]	0.493, 0.691, and 1.067 mm (circular) 0.494, 0.658, and 0.972 mm (square)	R134a	Horizontal	$G = 100$–$600\,\mathrm{kg/(m^2 \cdot s)}$ $q = 5$–$20\,\mathrm{kW/m^2}$ $T_{sat} = 40\,^{\circ}\mathrm{C}$ $x = 15$–85%	The flow condensation heat transfer coefficient increased with the refrigerant mass flux, and a clear increment in heat transfer coefficients was observed as the hydraulic diameter decreased. The flow condensation heat transfer coefficient increased with the refrigerant vapor quality, especially for high mass flux.

Table 1. *Continued*

Author	d	Fluids	Orientation/conditions	Range/applicability	Techniques, basis, observations
Cavallini et al. [31]	1.4 mm	R134a and R410A	Horizontal	$T_{sat} = 40\,^{\circ}C$ $x = 25\%$, 50%, and 75% $G = 200$–$1000\,kg/(m^2 \cdot s)$ for R134a tests $G = 200$–$1400\,kg/(m^2 \cdot s)$ for R410A tests	Experimental data are compared against models to show the accuracy of the models in the prediction of heat transfer coefficients inside minichannels.
Cavallini et al. [32]	0.4–3 mm	High pressure (R410A), medium (R134a), and low pressure (R236ea)	Horizontal		A new heat transfer model for condensation in minichannels with taking into account the effect of the entrainment rate of droplets from the liquid film.
Cavallini et al. [33]					A heat transfer model for condensation inside minichannels, based on analogy between heat and momentum transfer.
Wang and Rose [34]	0.5–5 mm	R134a, R22, and R410A	Horizontal square and equilateral triangular uniform wall temperature Saturated vapor at the inlet	$T_{sat} = 50\,^{\circ}C$	Presenting a theoretical model to predict film condensation heat transfer from a vapor flowing in horizontal square and equilateral triangular section minichannels or microchannels.
Bandhauer et al. [36]	0.506–1.524 mm	R134a	Horizontal	$G = 150$–$750\,kg/(m^2 \cdot s)$	The resulting heat transfer model predicted 86% of the data within ± 20%.
Cavallini et al. [39]	0.8 mm	R134a			The apparatus was designed for experimental tests both in condensation and vaporization, in a wide range of operating conditions and for a wide selection of refrigerants.
Chowdhury et al. [40]	0.7 mm	R134a	Horizontal	AR = 7 $T_{sat} = 30\,^{\circ}C$ $x = 20$–80% $G = 130$, $200\,kg/(m^2 \cdot s)$	A unique process for fabrication of the microchannel involving milling and electroplating steps was adopted to maintain the channel geometry close to design values.
Wang and Rose [41]	square (side 1 mm), triangular (side 1 mm), rectangular (sides 1 mm × 1.5 mm), and circular ($d = 1$ mm)	R134a	Horizontal uniform wall temperature	$G = 50\,kg/(m^2 \cdot s)$ $T_{sat} = 50\,^{\circ}C$	Studying effect of channel shape on film condensation in horizontal microchannels.
Garimella [42]	1 mm	R134a		$G = 300\,kg/(m^2 \cdot s)$ $x = 50\%$ $P = 1500\,kPa$	Comparing different techniques for predicting the heat transfer coefficients during condensation.
Jokar et al. [43]		R134a and 50% glycol–water mixture (counter-flow)			The two-phase theories and correlations that were established for conventional macrochannel heat exchangers might not hold for the minichannel heat exchangers.
Dessiatoun et al. [44]	0.7 mm	R134a, R245fa, and HFE7100			R245fa provided higher heat transfer coefficients compared to R134a with a significantly higher pressure drop in the minichannel.
Matkovic et al. [47]	0.96 mm	R134a and R32	Horizontal	$T_{sat} = 40\,^{\circ}C$ ($P_{sat} = 1017\,kPa$ for R134a and 2478 kPa for R32) $G = 100$–$1200\,kg/(m^2 \cdot s)$	Except for the lowest mass flux, the researchers did not find significant discrepancy from the trends expected for macroscale tubes.
Park and Hrnjak [48]	0.89 mm	CO_2	Horizontal	$T_{sat} = -15$, $-25\,^{\circ}C$ $G = 200$–$800\,kg/(m^2 \cdot s)$	Many correlations can predict the heat transfer coefficients within acceptable error range like the Cheng et al. [46] model.
Su et al. [52]		R134a and ammonia (NH_3)		$T_{sat} = 50\,^{\circ}C$ ($P_{sat} = 1.32\,MPa$ for R134a and 2.03 MPa for NH_3)	The heat transfer coefficient for ammonia might be around ten times those for R134a under similar conditions.
Matkovic et al. [53]	1.18 mm (square)	R134a	Horizontal	$T_{sat} = 40\,^{\circ}C$ $G = 200$–$800\,kg/(m^2 \cdot s)$	A heat transfer enhancement in the square minichannel at

Table 1. *Continued*

Author	d	Fluids	Orientation/conditions	Range/applicability	Techniques, basis, observations
					the lowest values of mass flux (due to the surface tension effect). No heat transfer coefficient increase at the highest values of the mass flux where condensation is shear stress dominated.
Marak [54]	1, 0.5, and 0.25 mm	CH_4, methane/ethane- and methane/nitrogen mixtures			The models concerning heat transfer and pressure drop in conventional channels can be used in tubes with diameter 1 mm and 0.5 mm while the results from the 0.25 mm tube are burdened with too high uncertainty to be used.
Huang et al. [55]	4.18 and 1.6 mm	R410A	Horizontal	$T_{sat} = 40\,^{\circ}C$ oil concentration = 0–5%	$\frac{h_{tp}d}{k_l} = 0.0152(-0.33 + 0.83\mathrm{Pr}_l^{0.8})* \frac{\phi_g}{X_{tt}}\mathrm{Re}_l^{0.77}$.
Agarwal and Garimella [56]	100–200 μm	R134a	Horizontal	$G = 200$–$800\,\mathrm{kg/(m^2 \cdot s)}$ $x = 0$–100% $T_{sat} = 30$, 40, 50, and 60 °C	The heat transfer increased with increasing vapor quality, increasing mass flux and decreasing saturation temperature.
Song et al. [57]	1.5 mm × 1.0 mm	FC72 and steam	Horizontal	$q = 130$–$170\,\mathrm{kW/m^2}$ for steam $q = 10$–$30\,\mathrm{kW/m^2}$ for FC72	Presenting preliminary results from a new research program for making accurate heat transfer and pressure drop measurements during condensation in microchannels.
Keinath and Garimella [58]	0.5–3 mm	R404a	Horizontal	$G = 200$–$800\,\mathrm{kg/(m^2 \cdot s)}$ $x = 5$–95% $T_{sat} = 30$–60 °C	Presenting a novel and accurate methodology for the quantitative investigation of two-phase flow regimes and flow parameters during condensation in minichannels.
Fronk and Garimella [59]	100–200 μm	CO_2	Horizontal	$G = 600\,\mathrm{kg/(m^2 \cdot s)}$ $x = 0$–100% $T_{sat} = 15$, 20 °C	Using the collected data to evaluate the applicability of correlations developed for larger hydraulic diameters and various fluids for predicting condensation heat transfer and pressure drop of CO_2.
Agarwal et al. [60]	0.424–0.839 mm	R134a	Horizontal barrel-shaped, N-shaped, rectangular, square, triangular, and W-shaped	$G = 150$–$750\,\mathrm{kg/(m^2 \cdot s)}$	The annular-flow-based model should be used for the square, barrel-shaped and rectangular channels, while the mist-flow correlation should be used for channels with sharp corners.
Del Col et al. [63]	0.96 mm	R1234yf	Horizontal	$G = 200$–$1000\,\mathrm{kg/(m^2 \cdot s)}$ $T_{sat} = 40\,^{\circ}C$	The heat transfer coefficients of R1234yf result to be lower as compared to the ones of R134a.
Kuo and Pan [64]	135 μm	Steam	Horizontal	2.10×10^{-6}–9.11×10^{-6} kg/s of steam for the uniform cross section microchannel 2.10×10^{-6}–5.93×10^{-6} kg/s of steam for the converging microchannel	The microchannels with the uniform cross section design have a higher heat transfer coefficient than those with the converging cross section under condensation in the mist/annular flow regimes.
Bortolin [66]	0.96 and 1.23 mm	R245fa, and R134a	Horizontal	$G = 67$–$789\,\mathrm{kg/(m^2 \cdot s)}$	Measuring the local heat transfer coefficients in circular and rectangular horizontal single microchannels made of copper during condensation.
Cavallini et al. [67]	0.96 mm	R32 and R245fa		$T_{sat} = 40\,^{\circ}C$ ($P_{sat} = 24.8$ bar for R32 and 2.5 bar for R245fa	The experimental values of the heat transfer coefficient show that the condensation is shear stress dominated for most of the data points, and in this range of operating conditions they can be well predicted by using the Cavallini et al. [68] model for macroscale condensation.
Goss et al. [69]	0.8 mm	R134a	Horizontal	$G = 57$–$125\,\mathrm{kg/(m^2 \cdot s)}$ $P = 6.8$–11.2 bar	The Yan and Lin [16] correlation gave the best results compared with the experimental data. For $x < 0.9$ (intermittent region on the Coleman and Garimella [70] map) this correlation fitted the experimental data very well, with a mean deviation of 13%.
Park et al. [71]	1.45 mm	R1234ze(E), R134a, and	Vertical	$G = 50$–$260\,\mathrm{kg/(m^2 \cdot s)}$ $T_{sat} = 25$–55 °C for R134a $T_{sat} = 30$–70 °C for R236fa and R1234ze(E)	$\frac{h_{tp}d_h}{k_l} = 0.0055\mathrm{Pr}_l^{1.37}\frac{\phi_g}{X_{tt}}\mathrm{Re}_l^{0.7}$.

Table 1. *Continued*

Author	d	Fluids	Orientation/conditions	Range/applicability	Techniques, basis, observations
Oh and Son [72]	1.77 mm	R236fa R22, R134a and R410 A	Horizontal	$G = 450–1050\ \mathrm{kg/(m^2 \cdot s)}$ $T_{sat} = 40\ ^\circ\mathrm{C}$	The condensation heat transfer coefficient of R410 A was higher than that of R22 and R134a at the given mass flux.
Bohdal et al. [74]	0.31–3.30 mm	R134a and R404A	Horizontal	$G = 100–1300\ \mathrm{kg/(m^2 \cdot s)}$ $x = 0–100\%$ $T_{sat} = 20–40\ ^\circ\mathrm{C}$	$\frac{h_{tp}d}{k_l} = 25.084\mathrm{Re}_l^{0.258}\mathrm{Pr}_l^{-0.495}\left(\frac{P}{P_{cr}}\right)^{-0.288} * \left(\frac{x}{1-x}\right)^{0.266}$
Wang and Rose [9]	0.5–2 mm	R134a, R22, R410A, NH_3, R152a, Propane (C_3H_8), CO_2	square, upright triangle, inverted triangle, rectangle	$G = 100–1300\ \mathrm{kg/(m^2 \cdot s)}$ $T_{sat} = 25—50\ ^\circ\mathrm{C}$	Presenting a theoretical model for condensation in microchannels with taking account of the influences of gravity and streamwise shear stress on the condensate surface as well as the transverse pressure gradient due to surface tension in the presence of change in condensate surface curvature.
Guermit [75]	0.8, 1.5, and 2 mm	R407d (R32/R125/R134a)		$U = 1$, 2, and 3 m/s	The heat transfer is enhanced by reducing the diameter of the minitube.
Alshqirate et al. [76]	0.6, 1.0, and 1.6 mm	CO_2		$\mathrm{Re_d} = 2000–15{,}000$	Using the dimensional analysis technique to develop correlations for Nusselt numbers and pressure drops.
Derby et al. [77]	1 mm	R134a	Horizontal square, triangular and semicircular	$G = 75–450\ \mathrm{kg/(m^2 \cdot s)}$ $P_{sat} = 887.5$ and 1176 kPa ($T_{sat} = 35$ and 45 °C) $q = 23.5$, 32, 46 $\mathrm{kW/m^2}$	The macroscale Shah [78] correlation best predicted their data, with a MAE of 20–30% for all geometries.
Kim and Mudawar [79]	1 mm	FC72 and water (counter flow)	Horizontal	For FC72, $G = 248–367\ \mathrm{kg/(m^2 \cdot s)}$ $T_{sat} = 57.8–62.3\ ^\circ\mathrm{C}$ $x = 23–100\%$ For water, mass flow rate = 3–6 g/s	Their new model accurately captured the heat transfer coefficient data in both magnitude and trend, evidenced by MAE values of 9.3%.
Kim and Mudawar [81]	1 mm	FC72 and water (counter flow)	Horizontal	For FC72, $G = 68–367\ \mathrm{kg/(m^2 \cdot s)}$ $T_{sat} = 57.2–62.3\ ^\circ\mathrm{C}$ $x = 0–100\%$ $q = 4.3–32.1\ \mathrm{kW/m^2}$ For water, $G = 69–138\ \mathrm{kg/(m^2 \cdot s)}$	A new condensation heat transfer coefficient correlation is proposed for annular condensation heat transfer in mini/microchannels. The new correlation shows excellent predictive capability based on both the present FC72 data and a large database for mini/microchannel flows amassed from eight previous sources.
Kuczyński et al. [84]	0.64, 0.90, 1.40, 1.44, 1.92, 2.30, and 3.30 mm	R134a and R404A	Horizontal		An unfavorable effect on the intensity of the heat transfer during the condensation process in pipe minichannels is identified in the range of frequencies, $f = 0.25–5$ Hz, of the periodically generated disturbances.
Fronk and Garimella [85]	1.435 mm	NH_3	Horizontal	$G = 75–150\ \mathrm{kg/(m^2 \cdot s)}$ $T_{sat} = 30$, 40, 50, 60 °C (corresponding to $P_r = 0.10–0.23$)	The coupled influences of ammonia properties and microscale geometry were outside the applicable range of most condensation heat transfer and pressure drop models. Additional reliable data heat transfer and pressure drop for smaller tube diameters and with working fluids like ammonia were necessary.
Da Riva and Del Col [86]	1 mm	R134a	Horizontal	$G = 100\ \mathrm{kg/(m^2 \cdot s)}$	Using the VOF method.The condensation process is gravity dominated, while the global effect of surface tension is negligible.
Nebuloni and Thome [87]	270 μm	R134a	focus on three external channel wall boundary conditions: a uniform wall temperature, a non-uniform wall heat flux, and single-phase convective cooling	$G = 300\ \mathrm{kg/(m^2 \cdot s)}$ $T_{sat} = 40\ ^\circ\mathrm{C}$ $x_{in} = 99.9\%$	Presenting numerical simulations of annular laminar film condensation heat transfer in microchannels of different internal shapes.
Zhang et al. [88]	1.088 and 1.289 mm	R22, R410A, and R407C	Horizontal	$G = 300–600\ \mathrm{kg/(m^2 \cdot s)}$ $T_{sat} = 30$, 40 °C $x = 10–90\%$	Wang et al. correlation [20] and Yan and Lin correlation [16] predicts the experimental data reasonably well. As a

Table 1. *Continued*

Author	d	Fluids	Orientation/conditions	Range/applicability	Techniques, basis, observations
					substitute for R22, R410A has more advantages than R407C in view of the characteristics of condensation heat transfer and pressure drop.
Del Col et al. [89]	1.23 mm	R134a	Horizontal, vertical downflow and 45 deg downwards	$G = 100$–$790\,\mathrm{kg/(m^2 \cdot s)}$ $T_{sat} = 40\,^{\circ}\mathrm{C}$	There is no differences for the three configurations at mass fluxes from 790 kg/(m^2 · s) down to 200 kg/(m^2 · s).
Del Col et al. [90]	1.23 mm	R134a	Horizontal, vertical downflow and vertical upflow	$G = 100$–$790\,\mathrm{kg/(m^2 \cdot s)}$ $T_{sat} = 40\,^{\circ}\mathrm{C}$	There is no differences for the three configurations at mass fluxes from 790 kg/(m^2 · s) down to 200 kg/(m^2 · s), where the condensation heat transfer is controlled by shear stress and surface tension.
Odaymet et al. [91]	$300 \times 310\,\mu$m	Steam	Horizontal		The local thermal performance of condensation flow in a microchannel is better for mist flow and upstream elongated bubble flow relative to slug and bubbly flows.
Hu et al. [92]		R134a, R32, R22, R123, R410A, and R1234yf		Database of 1183 condensation heat transfer data points of small channels from 11 independent research groups	The Koyama et al. [23] model could almost fit for all data under most of the operating conditions within an acceptable deviation.
Zhang et al. [93]	0.9 mm	CO_2		$T_{sat} = -5$ to $15\,^{\circ}\mathrm{C}$ $G = 180$, 360, and $540\,\mathrm{kg/(m^2 \cdot s)}$ $x = 20$–80%	The Thome et al. model [51] is applicable to the condenser under investigation, with deviation less than 30%.
Kim and Mudawar [94]	0.424–6.22 mm	17 various working fluids (R12, R123, R1234yf, R1234ze(E), R134a, R22, R236fa, R245fa, R32, R404A, R410A, R600a, FC72, methane, and CO_2)		$G = 53$–$1403\,\mathrm{kg/(m^2 \cdot s)}$ $\mathrm{Re_{lo}} = 276$–$89{,}798$ $x = 0$–100% $P_r = 0.04$–0.91	Proposing a new universal approach to predict the condensation heat transfer coefficient for mini/microchannel flows.
Goss and Passos [97]	0.77 mm	R134a	Horizontal	$G = 230$–$445\,\mathrm{kg/(m^2 \cdot s)}$ $P_{sat} = 7.3$–$9.7\,\mathrm{bar}$ $x = 55$–100% $q = 17$–$53\,\mathrm{kW/m^2}$	The mass flux and vapor mass quality have an important effect on the heat transfer coefficient.
Garimella and Fronk [98]	$0.1 < d_h < 5$ mm	Synthetic and natural refrigerants and their azeotropic and zeotropic mixtures			These experiments resulted in flow-regime-based heat transfer and pressure drop models with very good predictive capabilities for such microchannel geometries.
Wang and Rose [99]		R134a, NH_3	Laminar annular flow		The results of the annular flow theory are in surprisingly good agreement with the correlations when applied to R134a. For ammonia, the theoretical results lie between the widely spread values obtained from the correlations.
Liu et al. [100]	1.152 mm (circular)	R152a	Horizontal	$T_{sat} = 40$–$50\,^{\circ}\mathrm{C}$ $G = 200$–$1200\,\mathrm{kg/(m^2 \cdot s)}$ $x = 10$–90%	The heat transfer coefficients increased with mass flux and vapor quality while decreased with saturation temperature and heat flux. Inclination angle enhanced condensation heat transfer at low mass fluxes.

Table 1. *Continued*

Author	d	Fluids	Orientation/conditions	Range/applicability	Techniques, basis, observations
Liu et al. [101]	1.152 mm (circular) 0.952 mm (square)	R152a	Horizontal	$T_{sat} = 40–50\,^{\circ}C$ $G = 200–800\,kg/(m^2 \cdot s)$ $x = 10–90\%$	The heat transfer coefficients of the square microchannel are higher than those of the circular microchannel at $G = 200$ and $400\,kg/(m^2 \cdot s)$ due to the surface tension effect. The heat transfer enhancement decreases with mass flux as the shear stress plays a much more important role at higher mass fluxes.
Yun et al. [102]	0.68 mm	CO_2		oil concentrations (PAG type) = 0.7–1.2 wt.%	The heat transfer coefficient decreases with oil concentration. The heat transfer coefficient decreases by 50% as compared to that of the pure CO_2 when mass flux (G) was $600\,kg/(m^2 \cdot s)$, and oil concentration was changed from 0.7 to 1.2 wt.%.
Heo et al. [103]	1.5 mm	CO_2	Horizontal	$G = 400–1000\,kg/(m^2 \cdot s)$ $T_{sat} = -5$ to $5\,^{\circ}C$	The Thome et al. model [51] shows the smallest mean deviation of ±51.8% for the heat transfer coefficient.
El Achkar et al. [104]	The borosilicate channel of inner and outer edges 553 μm and 675 μm	n-pentane	Horizontal	$G = 3–15\,kg/(m^2 \cdot s)$	Investigation of flow patterns and heat transfer in a square cross section microcondenser working at low mass flux.
Ganapathy et al. [105]	100 μm	R134a	Constant heat flux	$G_g = 245–615\,kg/(m^2 \cdot s)$ $q = 200–800\,kW/m^2$	Using the VOF approach. The MAE is 16.6% for Nusselt number against the Dobson and Chato correlation [106].
Heo et al. [107]	1.5, 0.78, and 0.68 mm for the 7, 23, and 19 ports	CO_2	Horizontal	$G = 400–800\,kg/(m^2 \cdot s)$ $T_{sat} = -5$ to $5\,^{\circ}C$	The Thome et al. model [51] shows the smallest mean deviation of 47.7% for the heat transfer coefficient.
Rose and Wang [108]			Annular, laminar flow		Comparing detailed experimental investigations of condensation in microchannels where local heat flux and surface temperature were measured along the channel with theoretical results.
Dang and Doan [109]	375 μm and 265 μm				The condensation heat transfer coefficient in the microchannel heat exchangers decreased as increasing the inlet cooling water temperature.
Bortolin et al. [110]	1 mm	R134a	Steady state A uniform wall temperature is fixed as a boundary condition The liquid film and the vapor core are treated as turbulent	$G = 400, 800\,kg/(m^2 \cdot s)$	The VOF method is used to track the vapor–liquid interface, and the effects of interfacial shear stress, surface tension, and gravity are taken into account. The heat transfer mechanism is dominated by shear stress and surface tension.
Derby et al. [112]	1.06 mm	Steam	minichannel with hydrophobic and hydrophilic patterns	$G = 50–200\,kg/(m^2 \cdot s)$ $P = 350–400\,kPa$ $x = 20–95\%$	For the hydrophilic copper minigap, heat transfer coefficients are well predicted by Kim and Mudawar [94] correlation, with a MAE of 8.9%.
El Mghari et al. [113]	80–250 μm	Steam	Horizontal	$G = 80–160\,kg/(m^2 \cdot s)$	The correlation of Dobson et al. [114] and Koyama et al. [23] were the closest to the calculated steam condensation average heat transfer. The lowest average Nusselt numbers are obtained for the square microchannel.
Thome and Cioncolini [115]			Annular flow		Presenting unified modeling suite for annular flow, convective boiling and condensation in macrochannels and microchannels

condensation heat transfer was highlighted too. Thus, they obtained the lowest average Nusselt numbers for the square microchannel.

It is commonly accepted that there is no significant difference between forced convective evaporation and forced convective condensation, at least as long as nucleation at the channel wall is suppressed during the boiling process. As such, prediction methods designed for forced convective evaporation in the absence of wall nucleation could be applicable as well for forced convective condensation, and vice versa. As a result, Thome and Cioncolini [115] presented unified modeling suite for annular flow, convective boiling and condensation in macrochannels and microchannels. Annular flow is very important to the thermal design and simulation of micro-evaporators and microcondensers for two-phase cooling systems of high heat flux components for the thermal management of computer chips, power electronics, laser diodes and high energy physics particle detectors. First, the researchers presented unified suite of methods, illustrating in particular, the most recent updates. The annular flow suite included models in order to predict the void fraction, entrained liquid fraction, the wall shear stress and pressure gradient, and a turbulence model for momentum and heat transfer inside the annular liquid film. The turbulence model, in particular, allowed prediction of the local liquid film thicknesses and the local heat transfer coefficients during convective evaporation and condensation. The benefit of a unified modeling suite was that all the included prediction methods were consistently formulated and were proven to work well together, and provided a platform for continued advancement based on the other models in the suite. In convective condensation, the annular flow was established almost immediately at the inlet of channel and persisted over most of the condensation process until the condensate flooded the channel.

Table 1 presents a summary of the aforementioned previous studies on condensation heat transfer in microchannels and minichannels.

3 Recommendations for Future Studies

At the end, recommendations for future studies will be given. Although Kandlikar et al. [116] suggested in 2013 future research directions after reviewing the current state of research on heat transfer in microchannels including condensation, the present study will address different points, which were not included in the suggestions of future research directions in the study of Kandlikar et al. [116]. These new points will be expected to be the research focus in the coming years. Studying the heat transfer during the condensation process in microchannels and minichannels can be done using:

(1) The experiments with new types of noncircular shapes such as trapezoidal, elliptical, etc. To the best of the authors' knowledge, the study of heat transfer during the condensation process in microchannels and minichannels of elliptic cross section is not yet tackled in literature. Only recently a new interest has been devoted to the elliptical cross section, produced by mechanical fabrication in metallic microchannels for practical applications in MEMS. Also, the experimental study of the heat transfer during the condensation process in microchannels and minichannels can be done with the use of different triangular cross sections like right isosceles triangular.

(2) The experiments with new types of environmentally friendly refrigerants like HDR-14, which is low global warming fluid for replacement of R245fa. The GWP is an index used to compare the potential of gases to produce a greenhouse effect and the reference is CO_2 with a value of 1. HDR-14 has a GWP of only 7, much lower than the value of 930 of R245fa (both considering a period time horizon of 100 years). Also, HDR-14 has a much lower atmospheric life time (0.1 yr) in comparison with the atmospheric life time of R245fa (7.6 yr).

(3) The experiments with oil in the refrigerant loop (i.e., mixtures of refrigerants and oil) at different concentrations such as mixture of R134a with lubricant Castrol "icematic sw." The lubricant is synthetic polyol ester based oil commonly used in lubricating the compressors. This study is important because a common problem in a vapor compression refrigeration system is the mixing of small amounts of compressor lubricant in the refrigerant during the compression stages of the cycle. Then, this mixture becomes the working fluid and is responsible for the heat transfer in the cycle. It is believed that the mixing of the oil affects the performance of the condenser and thus influences the performance of the entire system. R134a in the refrigerant–oil mixture can be also replaced by R1234yf and R1234ze(E).

(4) The experiments with new kinds of refrigerant blends. For example, new refrigerant blends, such as R417 A, are becoming very important due to the possibility of using them in R22 systems with only minor changes (drop-in refrigerants) [117]. R417 A is the composition with mass fractions of 46.6% R125, 50% R134a, and 3.4% R600. Also, we can carry out the experiments with new kinds of refrigerant blends like R1234yf and R1234ze(E) as constituents as well as blends of old refrigerants with hydrofluoroolefin refrigerants. These blends can be azeotropic blends or zeotropic blends such as zeotropic mixture R32/R1234ze(E). R32 (CH_2F_2) is flammable and has for this reason not been used pure.

(5) Similar to recent work on condensation in macroscales at microgravity conditions [118,119], studies on condensation heat transfer in microchannels and minichannels at microgravity conditions can be done. These studies will be important because future manned space missions will be expected to greatly increase the space vehicle's size, weight, and heat dissipation requirements. An effective means to reducing both size and weight is replacing single-phase thermal management systems with two-phase counterparts that capitalize upon both sensible and latent heat of the coolant rather than sensible heat alone. This shift is expected to yield orders of magnitude enhancements in condensation heat transfer coefficients. A major challenge to this shift is the reliable tools lack for accurate prediction of two-phase pressure drop and heat transfer coefficient in reduced gravity. Developing such tools will require a sophisticated experimental facility to enable researchers to perform condensation experiments in microgravity in pursuit of reliable databases.

4 Summary and Conclusions

This paper provides a comprehensive, up-to-date review in a chronological order on the research progress made on condensation heat transfer in microchannels and minichannels. Also, studies on condensation heat transfer in microchannels and minichannels are summarized in Table 1. Finally, some suggestions for future work are presented. Therefore, the present study cannot only be used as the starting point for the researcher interested in condensation heat transfer in microchannels and minichannels, but it also includes recommendations for future studies on condensation heat transfer in microchannels and minichannels.

Acknowledgment

The second author wishes to thank King Mongkut's University of Technology Thonburi (KMUTT) for providing him with a post-doctoral fellowship. The third author wishes to thank the Thailand Research Fund, the Office of the Higher Education Commission and the National Research University Project for financial support of this study.

Nomenclature

AR = aspect ratio
Bo = Bond number

C = coefficient in Lockhart–Martinelli parameter
C_p = specific heat (J/(kg · K))
d = diameter (m)
Eu = Euler number
f = Fanning friction factor
g = gravitational acceleration (m/s^2)
G = mass flux (kg/(m^2 · s))
Ga = Galileo number
h = heat transfer coefficient (W/m^2 · K)
h_{lg} = latent heat of vaporization (J/kg)
J_g^* = dimensionless gas velocity = $xG/[gd_h\rho_g(\rho_l - \rho_g)]^{0.5}$
Ja = Jacob number
k = thermal conductivity (W/(m·K))
L = channel length (m)
Nu = Nusselt number
P = pressure (Pa)
Pr = Prantdl number
Re = Reynolds number
Su = Suratman number
T = temperature (°C)
U = velocity (m/s)
We = Weber number
We* = modified Weber number
x = mass quality
X = Lockhart–Martinelli parameter
Y = exponent

Greek Symbols

Δ = difference
μ = dynamic viscosity (kg/m · s)
ρ = density (kg/m^3)
σ = surface tension (N/m)
ϕ^2_g = two-phase frictional multiplier

Subscripts

ann = annular flow
av = average
cond = condenser
cr = critical
d = diameter
eq = equivalent
g = gas
go = gas phase with total mass flow rate
h = hydraulic
i = inner
in = inlet
l = liquid
lo = liquid phase with total mass flow rate
m = mean
nonann = slug and bubbly flow
tp = two-phase
tt = turbulent–turbulent
3 = based on three-sided heat transfer in rectangular channel
4 = based on four-sided heat transfer in rectangular channel

References

[1] Majumdar, A., Peterson, G. P., and Poulikakos, D., 2002, "Foreword," ASME J. Heat Transfer, **124**(2), pp. 221–222.
[2] Zhang, Z. M., and Mengüç, M. P., 2007, "Special Issue on Nano/Microscale Radiative Transfer," ASME J. Heat Transfer, **129**(1), pp. 1–2.
[3] Cheng, P., Choi, S., Jaluria, Y., Li, D., Norris, P., and Tzou, D. Y., 2009, "Special Issue on Micro/Nanoscale Heat Transfer—Part I," ASME J. Heat Transfer, **131**(3), p. 030301.
[4] Cheng, P., Choi, S., Jaluria, Y., Li, D., Norris, P., and Tzou, D. Y., 2009, "Special Issue on Micro/Nanoscale Heat Transfer—Part II," ASME J. Heat Transfer, **131**(4), p. 040301.
[5] Kandlikar, S. G., 2010, "Microchannels: Rapid Growth of a Nascent Technology," ASME J. Heat Transfer, **132**(4), p. 040301.
[6] Cheng, P., 2013, "Foreword to Special Issue on Micro/Nanoscale Heat and Mass Transfer," ASME J. Heat Transfer, **134**(5), p. 050301.
[7] Zhang, Z., Norris, P., and Peterson, G. P., 2013, "Foreword to Special Issue on Micro/Nanoscale Heat and Mass Transfer," ASME J. Heat Transfer, **135**(9), p. 090501.
[8] Kandlikar, S. G., 2003, "Microchannels and Minichannels—History, Terminology, Classification and Current Research Needs," ASME Paper No. ICMM2003-1000.
[9] Wang, H. S., and Rose, J. W., 2011, "Theory of Heat Transfer During Condensation in Microchannels," Int. J. Heat Mass Transfer, **54**(11–12), pp. 2525–2534.
[10] Yang, C.-Y., and Webb, R. L., 1996, "Condensation of R-12 in Small Hydraulic Diameter Extruded Aluminum Tubes With and Without Micro-Fins," Int. J. Heat Mass Transfer, **39**(4), pp. 791–800.
[11] Petukhov, B. S., 1970, "Heat Transfer and Friction in Turbulent Pipe Flow With Variable Physical Properties," Adv. Heat Transfer, **6**, pp. 503–564.
[12] Akers, W., Deans, O. K., and Crosser, O. K., 1959, "Condensation Heat Transfer Within Horizontal Tubes," Chem. Eng. Prog. Symp. Ser., **55**(29), pp. 171–176.
[13] Webb, R. L., and Zhang, M., 1998, "Heat Transfer and Friction in Small Diameter Channels," Microscale Thermophys. Eng., **2**(3), pp. 189–202.
[14] Moser, K. W., Webb, R. L., and Na, B., 1998, "A New Equivalent Reynolds Number Model for Condensation in Smooth Tubes," ASME J. Heat Transfer, **120**(2), pp. 410–417.
[15] Shah, M. M., 1979, "A General Correlation for Heat Transfer During Film Condensation in Tubes," Int. J. Heat Mass Transfer, **22**(4), pp. 547–556.
[16] Yan, Y. Y., and Lin, T. F., 1999, "Condensation Heat Transfer and Pressure Drop of Refrigerant R-134a in a Small Pipe," Int. J. Heat Mass Transfer, **42**(4), pp. 697–708.
[17] Webb, R. L., and Ermis, K., 2001, "Effect of Hydraulic Diameter on Condensation of R-134a in Flat, Extruded Aluminum Tubes," J. Enhanced Heat Transfer, **8**(2), pp. 77–90.
[18] Palm, B., 2001, "Heat Transfer in Microchannels," Microscale Thermophys. Eng., **5**(3), pp. 155–175.
[19] Zhao, T. S., and Liao, Q., 2002, "Theoretical Analysis of Film Condensation Heat Transfer Inside Vertical Mini Triangular Channels," Int. J. Heat Mass Transfer, **45**(13), pp. 2829–2842.
[20] Wang, W. W., Radcliff, R. N., and Christensen, R. N., 2002, "A Condensation Heat Transfer Correlation for Millimeter-Scale Tubing With Flow Regime Transition," Exp. Therm. Fluid Sci., **26**(5), pp. 473–485.
[21] Riehl, R. R., Ochterbeck, J. M., and Seleghim, P., Jr., 2002, "Effects of Condensation in Microchannels With a Porous Boundary: Analytical Investigation on Heat Transfer and Meniscus Shape," J. Braz. Soc. Mech. Sci. Eng., **24**(3), pp. 186–193.
[22] Riehl, R. R., and Ochterbeck, J. M., 2002, "Experimental Investigation of the Convective Condensation Heat Transfer in Microchannel Flows," Proceedings of the 9th Brazilian Congress of Thermal Engineering and Sciences (ENCIT 2002), Caxambu, Minas Gerais, Brazil, Oct. 15–18, Paper No. CIT02-0495.
[23] Koyama, S., Kuwahara, K., Nakashita, K., and Yamamoto, K., 2003, "An Experimental Study on Condensation of Refrigerant R134a in a Multi-Port Extruded Tube," Int. J. Refrig., **24**(4), pp. 425–432.
[24] Haraguchi, H., Koyama, S., and Fujii, T., 1994, "Condensation of Refrigerants HCFC22, HFC134a and HCFC123 in a Horizontal Smooth Tube (2nd Report, Proposal of Empirical Expressions for the Local Heat Transfer Coefficient)," Trans. Jpn. Soc. Mech. Eng., Ser. B, **60**(574), pp. 245–252.
[25] Mishima, K., and Hibiki, T., 1995, "Effect of Inner Diameter on Some Characteristics of Air-Water Two-Phase Flows in Capillary Tubes," Trans. Jpn. Soc. Mech. Eng., Ser. B, **61**(589), pp. 99–106.
[26] Garimella, S., 2004, "Condensation Flow Mechanisms in Microchannels: Basis for Pressure Drop and Heat Transfer Models," Heat Transfer Eng., **25**(3), pp. 104–116.
[27] Shin, J. S., and Kim, M. H., 2004, "An Experimental Study of Condensation Heat Transfer inside a Mini-Channel With a New Measurement Technique," Int. J. Multiphase Flow, **30**(3), pp. 311–325.
[28] Haui, X., and Koyama, S., 2004, "An Experimental Study of Carbon Dioxide Condensation in Mini Channels," J. Therm. Sci., **13**(4), pp. 358–365.
[29] Thome, J. R., 2004, "Condensation in Micro Channels," *Engineering Data Book III*, Wolverine Tube, Inc., Decatur, AL, Chap. 21.
[30] Shin, J. S., and Kim, M. H., 2005, "An Experimental Study of Flow Condensation Heat Transfer Inside Circular and Rectangular Mini-Channels," Heat Transfer Eng., **26**(3), pp. 36–44.
[31] Cavallini, A., Del Col, D., Doretti, L., Matkovic, M., Rossetto, L., and Zilio, C., 2005, "Condensation Heat Transfer and Pressure Gradient Inside Multiport Minichannels," Heat Transfer Eng., **26**(3), pp. 45–55.
[32] Cavallini, A., Doretti, L., Matkovic, M., and Rossetto, L., 2005, "Update on Condensation Heat Transfer and Pressure Drop Inside Minichannels," ASME Paper No. ICMM2005-75081.
[33] Cavallini, A., Doretti, L., Rossetto, L., Col, D. D., Matkovic, M., and Zilio, C., 2005, "A Model for Condensation Inside Minichannels," ASME Paper No. HT2005-72528.
[34] Wang, H. S., and Rose, J. W., 2005, "A Theory of Film Condensation in Horizontal Noncircular Section Microchannels," ASME J. Heat Transfer, **127**(10), pp. 1096–1105.
[35] Nusselt, W., 1916, "Die Oberflächenkondensation des Wasserdampfes," Z. Ver. Dt. Ing., **60**(27), pp. 541–546 and pp. 569–575.
[36] Bandhauer, T. M., Agarwal, A., and Garimella, S., 2006, "Measurement and Modeling of Condensation Heat Transfer Coefficients in Circular Microchannels," ASME J. Heat Transfer, **128**(10), pp. 1050–1059.
[37] Traviss, D. P., Rohsenow, W. M., and Baron, A. B., 1973, "Forced-Convection Condensation Inside Tubes: A Heat Transfer Equation for Condenser Design," ASHRAE Trans., **79**(1), pp. 157–165.

[38] Garimella, S., Agarwal, A., and Killion, J. D., 2005, "Condensation Pressure Drop in Circular Microchannels," Heat Transfer Eng., **26**(3), pp. 1–8.
[39] Cavallini, A., Del Col, D., Matkovic, M., and Rossetto, L., 2006, "Local Heat Transfer Coefficient During Condensation in a 0.8 mm Diameter Pipe," Proceedings of the 4th International Conference on Nanochannels, Microchannels and Minichannels (ICNMM2006), Limerick, Ireland, June 19–21, Vol. A, Paper No. ICNMM2006-96137, pp. 139–146.
[40] Chowdhury, S., Al-Hajri, E., Dessiatoun, S., Shooshtari, A., and Ohadi, M., 2006, "An Experimental Study of Condensation Heat Transfer and Pressure Drop in a Single High Aspect Ratio Micro-Channel for Refrigerant R134a," Proceedings of the 4th International Conference on Nanochannels, Microchannels and Minichannels (ICNMM2006), Limerick, Ireland, June 19–21, Vol. A, Paper No. ICNMM2006-96211, pp. 147–154.
[41] Wang, H. S., and Rose, J. W., 2006, "Film Condensation in Horizontal Microchannels: Effect of Channel Shape," Int. J. Therm. Sci., **45**(12), pp. 1205–1212.
[42] Garimella, S., 2006, "Condensation in Minichannels and Microchannels, Kandlikar," *Heat Transfer and Fluid Flow in Minichannels and Microchannels*, S. G., Garimella, S., Li, D. Colin, and S. M., King, eds., Elsevier, Oxford, UK.
[43] Jokar, A., Hosni, M. H., and Eckels, S. J., 2006, "Dimensional Analysis on the Evaporation and Condensation of Refrigerant R-134a in Minichannel Plate Heat Exchangers," Appl. Therm. Eng., **26**(17–18), pp. 2287–2300.
[44] Dessiatoun, S., Chowdhury, S., Al-hajri, E., Cetegen, E., and Ohadi, M., 2007, "Studies on Condensation of Refrigerants in a High Aspect Ratio Minichannel and in a Novel Micro-Groove Surface Heat Exchanger—Development of Micro-Condensers in Compact Two Phase Cooling Systems," Proceedings of the 5th International Conference on Nanochannels, Microchannels and Minichannels (ICNMM2007), Puebla, Mexico, June 18–20, pp. 109–116.
[45] Chen, Y., Shi, M., Cheng, P., and Peterson, G. P., 2008, "Condensation in Microchannels," Nanoscale Microscale Thermophy. Eng., **12**(2), pp. 117–143.
[46] Cheng, P., Wang, G., and Quan, X., 2009, "Recent Work on Boiling and Condensation in Microchannels," ASME J. Heat Transfer, **131**(4), p. 043211.
[47] Matkovic, M., Cavallini, A., Del Col, D., and Rossetto, L., 2009, "Experimental Study on Condensation Heat Transfer Inside a Single Circular Minichannel," Int. J. Heat Mass Transfer, **52**(9-10), pp. 2311–2323.
[48] Park, C. Y., and Hrnjak, P. S., 2009, "CO_2 Flow Condensation Heat Transfer and Pressure Drop in Multi-Port Microchannels at Low Temperatures," Int. J. Refrig., **32**(6), pp. 1129–1139.
[49] Akbar, M. K., Plummer, D. A., and Ghiaasiaan, S. M., 2003, "On Gas–Liquid Two-Phase Flow Regimes in Microchannels," Int. J. Multiphase Flow, **29**(5), pp. 855–865.
[50] Breber, G., Palen, J. W., and Taborek, J., 1980, "Prediction of Horizontal Tubeside Condensation of Pure Components Using Flow Regime Criteria," ASME J. Heat Transfer, **102**(3), pp. 471–476.
[51] Thome, J. R., El Hajal, J., and Cavallini, A., 2003, "Condensation in Horizontal Tubes, Part 2: New Heat Transfer Model Based on Flow Regimes," Int. J. Heat Mass Transfer, **46**(18), pp. 3365–3387.
[52] Su, Q., Yu, G. X., Wang, H. S., and Rose, J. W., 2009, "Microchannel Condensation: Correlations and Theory," Int. Refrig., **32**(6), pp. 1149–1152.
[53] Matkovic, M., Bortolin, S., Cavallini, A., and Del Col, D., 2009, "Experimental Study of Condensation Inside a Horizontal Single Square Minichannel," ASME Paper No. MNHMT2009-18258.
[54] Marak, K. A., 2009, "Condensation Heat Transfer and Pressure Drop for Methane and Binary Methane Fluids in Small Channels," Ph.D. thesis, Department of Energy and Process Engineering, Faculty of Engineering Science and Technology, Norwegian University of Science and Technology, Trondheim, Norway.
[55] Huang, X., Ding, G., Hu, H., Zhu, Y., Peng, H., Gao, Y., and Deng, B., 2010, "Influence of Oil on Flow Condensation Heat Transfer of R410A Inside 4.18 mm and 1.6 mm Inner Diameter Horizontal Smooth Tubes," Int. J. Refrig., **33**(1), pp. 158–169.
[56] Agarwal, A., and Garimella, S., 2010, "Representative Results for Condensation Measurements at Hydraulic Diameters ∼100 Microns," ASME J. Heat Transfer, **132**(4), p. 041010.
[57] Song, T. Y., Yu, G. X., Ma, X. H., Rose, J. W., and Wang, H. S., 2010, "Pressure Drop During Condensation in Microchannels," ASME Paper No. FEDSM-ICNMM2010-30230.
[58] Keinath, B. L., and Garimella, S., 2010, "Bubble and Film Dynamics During Condensation of Refrigerants in Minichannels," Proceedings of 2010 14th International Heat Transfer Conference (IHTC14), Washington, DC, Aug. 8–13, Vol. 2/Condensation, Paper No. IHTC14-22697, pp. 177–186.
[59] Fronk, B. M., and Garimella, S., 2010, "Measurement of Heat Transfer and Pressure Drop During Condensation of Carbon Dioxide in Microscale Geometries," Proceedings of 2010 14th International Heat Transfer Conference (IHTC14)," Washington, DC, Aug. 8–13, Vol. 2/Condensation, Paper No. IHTC14-22987, pp. 235–243.
[60] Agarwal, A., Bandhauer, T. M., and Garimella, S., 2010, "Measurement and Modeling of Condensation Heat Transfer in Non-Circular Microchannels," Int. J. Refrig., **33**(6), pp. 1169–1179.
[61] Agarwal, A., and Garimella, S., 2009, "Modeling of Pressure Drop During Condensation in Circular and Noncircular Microchannels," ASME J. Fluids Eng., **131**(1), p. 011302.
[62] Soliman, H. M., 1986, "The Mist-Annular Transition During Condensation and Its Influence on the Heat Transfer Mechanism," Int. J. Multiphase Flow, **12**(2), pp. 277–288.
[63] Del Col, D., Torresin, D., and Cavallini, A., 2010, "Heat Transfer and Pressure Drop During Condensation of the Low GWP Refrigerant R1234yf," Int. J. Refrig., **33**(7), pp. 1307–1318.
[64] Kuo, C. Y., and Pan, C., 2010, "Two-Phase Flow Pressure Drop and Heat Transfer During Condensation in Microchannels With Uniform and Converging Cross-Sections," J. Micromech. Microeng., **20**(9), p. 095001.
[65] Kuo, C. Y., and Pan, C., 2010, "The Effect of Cross-Section Design of Rectangular Microchannels on Convective Steam Condensation," J. Micromech. Microeng., **19**(3), p. 035017.
[66] Bortolin, S., 2010, "Two-Phase Heat Transfer Inside Minichannels," Ph.D. thesis, University of Padua, Padova, Italy.
[67] Cavallini, A., Bortolin, S., Del Col, D., Matkovic, M., and Rossetto, L., 2011, "Condensation Heat Transfer and Pressure Losses of High and Low Pressure Refrigerants Flowing in a Single Circular Minichannel," Heat Transfer Eng., **32**(2), pp. 90–98.
[68] Cavallini, A., Censi, G., Del Col, D., Doretti, L., Matkovic, M., Rossetto, L., and Zilio, C., 2006, "Condensation in Horizontal Smooth Tubes: A New Heat Transfer Model for Heat Exchanger Design," Heat Transfer Eng., **27**(8), pp. 31–38.
[69] Goss, G., Jr., Macarini, S. F., and Passos, J. C., 2011, "Heat Transfer and Pressure Drop During Condensation of R-134A Inside Parallel Microchannels," ASME Paper No. AJTEC2011-44551.
[70] Coleman, J. W., and Garimella, S., 2000, "Two-Phase Flow Regime Transitions in Microchannel Tube: The Effect of Hydraulic Diameter," ASME Heat Transfer Division, **366**(4), pp. 71–83.
[71] Park, J. E., Vakili-Farahani, F., Consolini, L., and Thome, J. R., 2011, "Experimental Study on Condensation Heat Transfer in Vertical Minichannels for New Refrigerant R1234ze(E) Versus R134a and R236fa," Exp. Therm. Fluid Sci., **35**(3), pp. 442–454.
[72] Oh, H.-K., and Son, C.-H., 2011, "Condensation Heat Transfer Characteristics of R-22, R-134a and R-410A in a Single Circular Microtube," Exp. Therm. Fluid Sci., **35**(4), pp. 706–716.
[73] Gnielinski, V., 1976, "New Equations for Heat and Mass Transfer in Turbulent Pipe and Channel Flow," Int. Chem. Eng., **16**(2), pp. 359–368.
[74] Bohdal, T., Charun, H., and Sikora, M., 2011, "Comparative Investigations of the Condensation of R134a and R404A Refrigerants in Pipe Minichannels," Int. J. Heat Mass Transfer, **54**(9–10), pp. 1963–1974.
[75] Guermit, T., 2011, "Simulation Study of the Condensation of Mixed Refrigerant R407d (R32/R125/R134a)," J. Appl. Sci. Environ. Sanit., **6**(2), pp. 105–113.
[76] Alshqirate, A. A. Z. S., Tarawneh, M., and Hammad, M., 2012, "Dimensional Analysis and Empirical Correlations for Heat Transfer and Pressure Drop in Condensation and Evaporation Processes of Flow Inside Micropipes: Case Study With Carbon Dioxide (CO_2)," J. Braz. Soc. Mech. Sci. Eng., **34**(1), pp. 89–96.
[77] Derby, M., Lee, H. J., Peles, Y., and Jensen, M. K., 2012, "Condensation Heat Transfer in Square, Triangular and Semicircular Mini-Channels," Int. J. Heat Mass Transfer, **55**(1-3), pp. 187–197.
[78] Shah, M. M., 2009, "An Improved and Extended General Correlation for Heat Transfer During Condensation in Plain Tubes," HVAC&R Res., **15**(5), pp. 889–913.
[79] Kim, S. M., and Mudawar, I., 2012, "Theoretical Model for Annular Flow Condensation in Rectangular Microchannels," Int. J. Heat Mass Transfer, **55**(4), pp. 958–970.
[80] Kim, S. -M., Kim, J., and Mudawar, I., 2012, "Flow Condensation in Parallel Micro-Channels—Part 1: Experimental Results and Assessment of Pressure Drop Correlations," Int. J. Heat Mass Transfer, **55**(4), pp. 971–983.
[81] Kim, S.-M., and Mudawar, I., 2012, "Flow Condensation in Parallel Micro-Channels—Part 2: Heat Transfer Results and Correlation Technique," Int. J. Heat Mass Transfer, **55**(4), pp. 984–994.
[82] Shah, R. K., and London, A. L., 1978, "Advances in Heat Transfer," *Laminar Forced Flow Convection in Ducts, Suppl. 1*, Academic Press, New York.
[83] Cavallini, A., Censi, G., Col, D. D., Doretti, L., Longo, G. A., and Rossetto, L., 2002, "Condensation of Halogenated Refrigerants Inside Smooth Tubes," HVAC&R Res., **8**(4), pp. 429–451.
[84] Kuczyński, W., Charun, H., and Bohdal, T., 2012, "Influence of Hydrodynamic Instability on the Heat Transfer Coefficient During Condensation of R134a and R404A Refrigerants in Pipe Mini-Channels," Int. J. Heat Mass Transfer, **55**(4), pp. 1083–1094.
[85] Fronk, B. M., and Garimella, S., 2012, "Heat Transfer and Pressure Drop During Condensation of Ammonia in Microchannels," ASME Paper No. MNHMT2012-75265.
[86] Da Riva, E., and Del Col, D., 2012, "Numerical Simulation of Laminar Liquid Film Condensation in a Horizontal Circular Minichannel," ASME J. Heat Transfer, **134**(5), p. 051019.
[87] Nebuloni, S., and Thome, J. R., 2012, "Numerical Modeling of the Conjugate Heat Transfer Problem for Annular Laminar Film Condensation in Microchannels," ASME J. Heat Transfer, **134**(5), p. 051021.
[88] Zhang, H.-Y., Li, J.-M., Liu, N., and Wang, B.-X., 2012, "Experimental Investigation of Condensation Heat Transfer and Pressure Drop of R22, R410A and R407C in Mini-Tubes," Int. J. Heat Mass Transfer, **55**(13–14), pp. 3522–3532.
[89] Del Col, D., Bortolato, M., Bortolin, S., and Cavallini, A., 2012, "Experimental Study of Condensation inside a Square Minichannel: Effect of Channel Orientation," 8th ECI International Conference on Boiling and Condensation Heat Transfer, Ecole Polytechnique Fédérale de Lausanne (EPFL), Lausanne, Switzerland, June 3–7.
[90] Del Col, D., Bortolato, M., Bortolin, S., and Azzolin, M., 2012, "Minichannel Condensation in Downward, Upward and Horizontal Configuration," J. Phys.: Conf. Ser., **395**(1), p. 012092.

[91] Odaymet, A., Louahlia-Gualous, H., and De Labachelerie, M., 2012, "Local Heat Transfer and Flow Patterns During Condensation in a Single Silicon Microchannel," Nanoscale Microscale Thermophys. Eng., **16**(4), pp. 220–241.
[92] Hu, C., Li, M., Ma, Y., and Fu, X., 2012, "Analysis of Condensation Heat Transfer Model in Small Channels," Jixie Gongcheng Xuebao/J. Mech. Eng., **48**(24), pp. 134–140.
[93] Zhang, Z., Weng, Z. L., Li, T. X., Huang, Z. C., Sun, X. H., He, Z. H., van Es, J., Pauw, A., Laudi, E., and Battiston, R., 2013, "CO_2 Condensation Heat Transfer Coefficient and Pressure Drop in a Mini-Channel Space Condenser," Exp. Therm. Fluid Sci., **44**, pp. 356–363.
[94] Kim, S. -M., and Mudawar, I., 2013, "Universal Approach to Predicting Heat Transfer Coefficient for Condensing Mini/Micro-Channel Flow," Int. J. Heat Mass Transfer, **56**(1–2), pp. 238–250.
[95] Churchill, S. W., and Usagi, R., 1972, "A General Expression for the Correlation of Rates of Transfer and Other Phenomena," Am. Inst. Chem. Eng. J., **18**(6), pp. 1121–1128.
[96] Awad, M. M., 2014, "Prediction of Wall Friction Factor in Horizontal Annular Flow Using the Asymptotic Method," Ann. Nucl. Energy, **65**, pp. 308–313.
[97] Goss, G., Jr., and Passos, J. C., 2013, "Heat Transfer During the Condensation of R134a Inside Eight Parallel Microchannels," Int. J. Heat Mass Transfer, **59**, pp. 9–19.
[98] Garimella, S., and Fronk, B. M., 2013, "Single- and Multi-Constituent Condensation of Fluids and Mixtures With Varying Properties in Micro-Channels," Exp. Heat Transfer, **26**(2-3), pp. 129–168.
[99] Wang, H. S., and Rose, J. W., 2013, "Heat Transfer and Pressure Drop During Laminar Annular Flow Condensation in Micro-Channels," Exp. Heat Transfer, **26**(2–3), pp. 247–265.
[100] Liu, N., Wang, X.-Y., and Li, J.-M., 2013, "Experimental Investigation on Heat Transfer of R152a During Condensation in a Circular Microchannel," Kung Cheng Je Wu Li Hsueh Pao/J. Eng. Thermophys., **34**(3), pp. 517–521.
[101] Liu, N., Li, J. M., Sun, J., and Wang, H. S., 2013, "Heat Transfer and Pressure Drop during Condensation of R152a in Circular and Square Microchannels," Exp. Therm. Fluid Sci., **47**, pp. 60–67.
[102] Yun, R., Park, H., and Hwang, Y., 2013, "Inflow Condensation Heat Transfer Characteristics of CO_2 in Microchannel," 8th International Conference on Multiphase Flow (ICMF 2013), Category: Multiphase Flow in Heat and Mass Transfer, Jeju, Korea, Vol. 8, May 26–31, 2013, Paper No. ICMF2013-082.
[103] Heo, J., Park, H., and Yun, R., 2013, "Condensation Heat Transfer and Pressure Drop Characteristics of CO_2 in a Microchannel," Int. J. Refrig., **36**(6), pp. 1657–1668.
[104] El Achkar, G., Miscevic, M., Lavieille, P., Lluc, J., and Hugon, J., 2013, "Flow Patterns and Heat Transfer in a Square Cross-Section Micro Condenser Working at Low Mass Flux," Appl. Therm. Eng., **59**(1-2), pp. 704–716.
[105] Ganapathy, H., Shooshtari, A., Choo, K., Dessiatoun, S., Alshehhi, M., and Ohadi, M., 2013, "Volume of Fluid-Based Numerical Modeling of Condensation Heat Transfer and Fluid Flow Characteristics in Microchannels," Int. J. Heat Mass Transfer, **65**, pp. 62–72.
[106] Dobson, M. K., and Chato, J. C., 1998, "Condensation in Smooth Horizontal Tubes," ASME J. Heat Transfer, **120**(1), pp. 193–213.
[107] Heo, J., Park, H., and Yun, R., 2013, "Comparison of Condensation Heat Transfer and Pressure Drop of CO_2 in Rectangular Microchannels," Int. J. Heat Mass Transfer, **65**, pp. 719–726.
[108] Rose, J., and Wang, H., 2013, "Microchannel Condensation—Comparisons of Annular Laminar Flow Theory With Detailed Measurements," ASME Paper No. MNHMT2013-22156.
[109] Dang, T., and Doan, M., 2013, "An Experimental Investigation on Condensation Heat Transfer of Microchannel Heat Exchangers," Int. J. Comput. Eng. Res., **3**(12), pp. 25–31.
[110] Bortolin, S., Da Riva, E., and Del Col, D., 2014, "Condensation in a Square Minichannel: Application of the VOF Method," Heat Transfer Eng., **35**(2), pp. 193–203.
[111] Menter, F. R., 1994, "Two-Equation Eddy-Viscosity Turbulence Models for Engineering Applications," AIAA J., **32**(8), pp. 1598–1605.
[112] Derby, M. M., Chatterjee, A., Peles, Y., and Jensen, M. K., 2014, "Flow Condensation Heat Transfer Enhancement in a Mini-Channel With Hydrophobic and Hydrophilic Patterns," Int. J. Heat Mass Transfer, **68**, pp. 151–160.
[113] El Mghari, H., Asbik, M., Louahlia-Gualous, H., and Voicu, I., 2014, "Condensation Heat Transfer Enhancement in a Horizontal Non-Circular Microchannel," Appl. Therm. Eng., **64**(1–2), pp. 358–370.
[114] Dobson, M. K., Chato, J. C., Hinde, D. K., and Wang, S. P., 1994, "Experimental Evaluation of Internal Condensation of Refrigerants R-12 and R-134a," ASHRAE Trans., **100**(1), pp. 744–754.
[115] Thome, J. R., and Cioncolini, A., 2014, "Unified Modeling Suite for Two-Phase Flow, Convective Boiling and Condensation in Macro- and Micro-Channels," Proceedings of the Fourth Micro and Nano Flows Conference (MNF2014), University College London (UCL), London, UK, Sept. 7–10.
[116] Kandlikar, S. G., Colin, S., Peles, Y., Garimella, S., Pease, R. F., Brandner, J. J., and Tuckerman, D. B., 2013, "Heat Transfer in Microchannels—2012 Status and Research Needs," ASME J. Heat Transfer, **135**(9), p. 091001.
[117] Pardiñas, Á. Á., Fernández-Seara, J., Piñeiro-Pontevedra, C., and Bastos, S., 2014, "Experimental Determination of the Boiling Heat Transfer Coefficients of R-134a and R-417A on a Smooth Copper Tube," Heat Transfer Eng., **35**(16–17), pp. 1427–1434.
[118] Lee, H., Mudawar, I., and Hasan, M. M., 2013, "Experimental and Theoretical Investigation of Annular Flow Condensation in Microgravity," Int. J. Heat Mass Transfer, **61**, pp. 293–309.
[119] Lee, H., Park, I., Konishi, C., Mudawar, I., May, R. I., Juergens, J. R., Wagner, J. D., Hall, N. R., Nahra, H. K., Hasan, M. M., and Mackey, J. R., 2014, "Experimental Investigation of Flow Condensation in Microgravity," ASME J. Heat Transfer, **136**(2), p. 021502.